

PREDICTIVE DIRECT POWER CONTROL OF VOLTAGE SOURCE CONVERTER (VSC) IN MICROGRIDS

BY

AFTAB AHMED

01-244171-039

SUPERVISED BY

DR. ASAD WAQAR



Session-2017-2019

A Report submitted to the Department of Electrical Engineering
Bahria University, Islamabad
in partial fulfilment of the requirement for the degree of MS (EE)

CERTIFICATE

We accept the work contained in this report as a confirmation to the required standard for the partial fulfilment of the degree of MS (EE).

Head of Department

Supervisor

Internal Examiner

External Examiner

DEDICATION

I dedicate my work to my loving parents without them I am nothing. My supervisor who made me motivated during the entire time of this thesis. My humble efforts during the completion of this thesis and report are dedicated to my parents, friends and teachers who give a lot of guidance, supervision, assistance and support to me.

DECLARATION OF AUTHORSHIP

I hereby state that content of this thesis is my own work and that it is the result of work done during the period of registration. To the best of my knowledge, it contains no material previously published or written by another person nor material which to a substantial extent has been accepted for the award of any other degree or diploma of the university or other institute of higher learning, except where due acknowledgement has been made in the text.

ACKNOWLEDGEMENTS

“In the name of Allah, the most gracious, the most merciful”

Without the help and guidance of Almighty Allah who is the source of complete knowledge and wisdom to all the mankind it was not possible for me to complete the thesis.

The completion of this thesis was possible only because of the cooperation, guidance and patience of our parents, friends and teachers.

I have no words to express my deepest thanks and regard to Dr. Asad Waqar whose guidance, patience and helpful suggestions helped me a lot during this thesis. I would like to say that without the kind and helpful supervision and assistance of our beloved supervisor Dr. Asad Waqar it was not possible for me to complete this report and thesis.

I would also like to thank my seniors and friends especially Hussain Sarwar and Tasawar Abbas who helped a lot whenever I faced difficulties.

ABSTRACT

In recent years, electricity generation from standard fossil fuel resources originate critical influence on the environment. Moreover, fossil fuel resources are evacuating day by day. Therefore, the microgrid is an effective way of integrating current power system and renewable energy resources. A microgrid is a type of grid that has local distributed generators (DGs) and it is connected to the national grid but also able to work independently and have effective control. Hybrid AC/DC microgrid, DC microgrid and AC microgrid and are the three categories of microgrid. The generally used configuration in the AC microgrid because it provides a straightforward way for the integration of DG modules and existing network utilities with minimal modifications. Although maximum distribution networks are AC, ESS units, addition of DC modules and DG-based loads is included. More characteristics include opening the entryways of distribution networks which are based on DC. The features of both AC and DC are combined in hybrid AC/DC microgrid. In hybrid microgrid, the three phase AC/DC bidirectional converter is required for power conversion. It can operate both in rectification mode and inverter mode. In rectification mode, it can regulate power on the DC side or it can maintain voltage on the DC side. In inverter mode, it can further operate in two modes, islanded mode and grid connected mode. In grid connected mode, national grid controls the frequency and voltage of the microgrid while power is control by the DG. In the islanded mode, DG control the frequency and voltage of a microgrid and also fulfill the local demand. Bidirectional Voltage Source converter (VSC) is an essential component in hybrid microgrids. The challenges in bidirectional converter are; control of power flow in both directions while maintaining stability, efficient transitions between the modes and efficient control of non-linearity. This study proposes the FCS–MPC control scheme for the bidirectional converter in hybrid microgrid. In the proposed scheme, future value of the system at each sampling instant is forecasted for every switching states using system’s mathematical model. After this, for the next sampling instant optimum action is applied using cost function. Converter switching frequency is reduced using tow-step horizon-based cost function (CF). The proposed MPC model for bidirectional converter is verified for its robustness and effectiveness using MATLAB/SIMULINK.

Table of Contents

Contents

Certificate.....	i
Dedication.....	ii
Declaration of Authorship.....	iii
Acknowledgements.....	iv
ABSTRACT.....	v
LIST OF TABLES.....	viii
LIST OF FIGURES.....	ix
ABBREVIATIONS.....	xi
CHAPTER 1. INTRODUCTION.....	2
1.1. Problem Description:.....	5
1.2. Thesis Objectives:.....	6
1.3. Thesis Organization:.....	6
CHAPTER 2. LITERATURE REVIEW.....	8
2.1. Classical Control Methods:.....	8
2.1.1. Voltage Oriented Control:.....	8
2.1.2. Direct Power Control (DPC) and Direct Torque Control (DTC):.....	9
2.1.3. Drawbacks in Linear Controllers:.....	9
2.2. Non Linear Control Techniques:.....	10
2.2.1. Hysteresis Control:.....	10
2.2.2. Sliding Mode Control (SMC):.....	10
2.2.3. Other Non Linear Control Techniques:.....	11
2.2.4. Model Predictive Control:.....	11
CHAPTER 3. METHODOLOGY.....	19
3.1. Mathematical Modeling and Description of the system:.....	19
3.1.1. Finite Control Set Model Predictive Control (FCS-MPC):.....	19
3.1.2. Control of an Active Front End Rectifier:.....	26
3.2. Voltage Model Predictive Control in Islanded Mode:.....	35
3.3. Direct Power Model Predicted Control in Grid Connected Mode:.....	41
CHAPTER 4. RESULTS.....	48
4.1. Bidirectional VSC as Active Front End (AFE) Rectifier:.....	49

4.1.1. Regulation of DC link Voltage.....	49
4.1.2. Step Change in DC link Voltage:	51
4.1.3. Regulation of Load:	52
4.1.4. Regulation of power/Step Change in Power:	53
4.2. Bidirectional VSC as Voltage Source Inverter (Grid Connected Mode):	54
4.2.1. Regulation of Power/Step Change in Power:	54
4.2.2. Unbalanced Linear load:.....	56
4.3. Bidirectional VSC as Voltage Source Inverter (Islanded Mode):	57
4.3.1. Regulation of voltage and frequency:.....	57
4.3.2. Step Change in Linear Load:	58
4.3.3. Non Linear Load:.....	59
4.4. Transitions between modes of microgrid:	60
4.5. Comparative Analysis:	61
CHAPTER 5. CONCLUSIONS AND FUTURE WORK.....	64
5.1. CONCLUSION:	64
5.2. FUTURE WORK:	64
References.....	65

LIST OF TABLES

Table 2.1 Comparison between Non-linear & linear control technique.	16
Table 2.2 Comparison between PI & MPC Control.	16
Table 3.1 Voltage Space vector of Bidirectional AC-DC Bidirectional Converter.....	24
Table 3.2 Switching State Definition.....	24
Table 4.1 Parameters for the simulations.....	48
Table 4.2 % THD.....	61
Table 4.3 Comparison between Conventional and Proposed Scheme (Inverter Mode).....	61
Table 4.4 Comparison between different control methods (Inverter Mode)	62

LIST OF FIGURES

Figure 1.1 AC Microgrid	3
Figure 1.2 DC Microgrid	4
Figure 1.3 Hybrid Microgrid.....	5
Figure 2.1 Types of Predictive Controllers.....	17
Figure 3.1 Principle of MPC.....	20
Figure 3.2 Block Diagram of MPC.....	21
Figure 3.3 Three Phase Bidirectional AC-DC Converter Topology.....	22
Figure 3.4 Space Vector Modulation	25
Figure 3.5 Voltage Vectors Generated by VSC.....	25
Figure 3.6 Rectifier Topologies	28
Figure 3.7 AFE Model	29
Figure 3.8 Predictive Power Control	33
Figure 3.9 Active Front End (AFE) Rectifier Flowchart.....	34
Figure 3.10 VMPC Flowchart.....	40
Figure 3.11 DPMPC Flowchart	46
Figure 4.1 Simulation results of bidirectional VSC in Rectification mode: (a) DC link Voltage (b) Three phase grid Voltage (V) and Three Phase AC Grid Current (A).....	50
Figure 4.2 Simulation results of bidirectional VSC in Rectification mode: Step change in DC link Voltage from 500V to 350V at 0.5sec	51
Figure 4.3 Simulation results of bidirectional VSC in Rectification mode: (a) Step change in load from 50 ohm to 100 ohm at 0.5sec (b) Three Phase grid Voltage (V) and Three Phase grid Current (A).....	52
Figure 4.4 Simulation results of bidirectional VSC in Rectification mode: (a)Regulation of power/Step change in power on DC side from $P = 1\text{KW}$ to 1.5KW , $Q = 0\text{VAR}$ (b) (b) Three Phase grid Voltage (V) and Three Phase grid Current (A).....	53
Figure 4.5 Simulation results of bidirectional VSC in Inverter (Grid Connected Mode): (a) Regulation of power/Step change in Power $P = 10\text{KW}$, $Q = 0\text{VAR}$ to $P = 15\text{KW}$, $Q = 10\text{kVAR}$ (b) Three Phase AC Voltage (V) and Three Phase AC Current (A).....	55
Figure 4.6 Simulation results of bidirectional VSC in Inverter (Grid Connected Mode): (a) Regulation of power $P = 10\text{KW}$, $Q = 0\text{VAR}$ (b) Three Phase AC Voltage (V) and Three Phase AC Current (A)	56
Figure 4.7 Simulation results of bidirectional VSC in Inverter (Islanded Mode): Three phase AC Grid Voltage and Three phase AC Grid Current (A) x10.....	57
Figure 4.8 Simulation results of bidirectional VSC in Inverter (Islanded Mode): Three phase AC Grid Voltage and Three phase AC Grid Current (A) x10 for step change of load from 50 ohm to 100 ohm at 0.5sec	58
Figure 4.9 Simulation results of bidirectional VSC in Inverter (Islanded Mode): Three phase AC Grid Voltage (V) and Three phase AC Grid Current (A) x10 when there is transition from linear load (50 ohm) to non linear load at 0.5sec.....	59

Figure 4.10 Simulation results of bidirectional VSC when there is transition between rectification mode and inverter mode: Three phase AC grid Voltage (V) and Three phase AC grid Current (A)
..... 60

ABBREVIATIONS

DPMPC	Direct Power Model Predictive control
DPC	Direct Power Control
DTC	Direct Torque Control
FCS-MPC	Finite control set- model predictive control
CF	Cost Function
MPC	Model predictive control
VMPC	Voltage Model Predictive Control
VSC	Voltage Source Converter

Chapter 1

Introduction

CHAPTER 1. INTRODUCTION

In past few years, electricity generation from standard fossil fuel resources originate critical influence on the environment. Moreover, fossil fuel resources are evacuating day by day. This has created need of generating electricity from the resources that are good for the environment like renewable resources. Wind, solar and hydropower are different forms of RE resources. Although, the RE resources are intermittent in nature which constitute a technical problems in their integration with the current power system. Therefore, the microgrid is an effective way of integrating current power system and renewable energy resources.

A microgrid is a type of grid that has local distributed generators (DGs) and it is connected to the national grid but also able to work independently and have effective control [1], [2]. Hybrid AC/DC microgrid, DC microgrid and AC microgrid are the three categories of microgrid. [3], [4], [5], [6]-13].

The AC microgrid is generally used arrangement because it offers a straightforward way for the integration of DG modules and existing network utilities with minimal modifications as shown in figure 1.1. This structure is characterized to facilitate the adjustment of low voltage levels frequency transformers and have a high level of error handling - detect errors and correct them. Although, it has some disadvantages, such as synchronization of DG modules, interactive energy rotation, which increases the energy lost in the transport system [14], [15], [16], and [17].

Although maximum distribution networks are AC, ESS units, addition of DC modules and DG-based loads is included. More characteristics include opening the entryways of distribution networks which are based on DC. Higher efficiency is its main advantage and there is no reactive power in the network. More, synchronization of DG modules is not needed. Although, this arrangement requires a large refinement of the energy distribution network. Therefore considerably increases the costs [18], [19], [20], [21], [22], [23]. Figure 1.2 shows the Dc microgrid.

The features of both DC and AC are combined in hybrid DC/AC microgrid. [24], [25], [26], [27], and as shown in figure 1.3 [28]. The distribution network itself allows direct integration of ESS

loads, DC and AC based DG as well as AC and DC loads. This characteristics provides an effective path to integrate RES or EV electric vehicles with minimal modification to the current network. So overall cost will be reduced. Hybrid DC / AC microgrids are an excellent way for joining smart grids with traditional distribution.

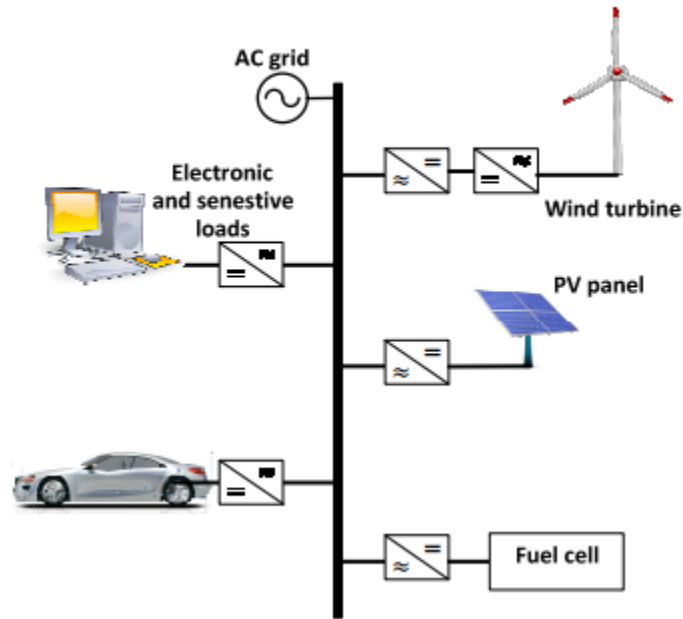


Figure 1.1 AC Microgrid

A three phase bidirectional AC / DC converter is required in hybrid microgrids for power conversion as shown in figure 1.3. It can work both rectification mode and inverter mode. In rectification mode regulate power on the DC side or it can maintain voltage on the DC side. In inverter mode, it can further operate in two modes, islanded mode and grid connected mode. In the grid connected mode, national grid controls the frequency and voltage of the microgrid while power is control by the DG. In the islanded mode, DG control the frequency (Hz) and voltage(V) of a microgrid and also fulfill the local demand [29]. To prevent the poor quality problems like AC Voltage distortion, low power factor, total harmonic problems (THD), DC voltage pulsations and ripple in DC current, the bidirectional AC/DC converter should be very efficient [30], [31].

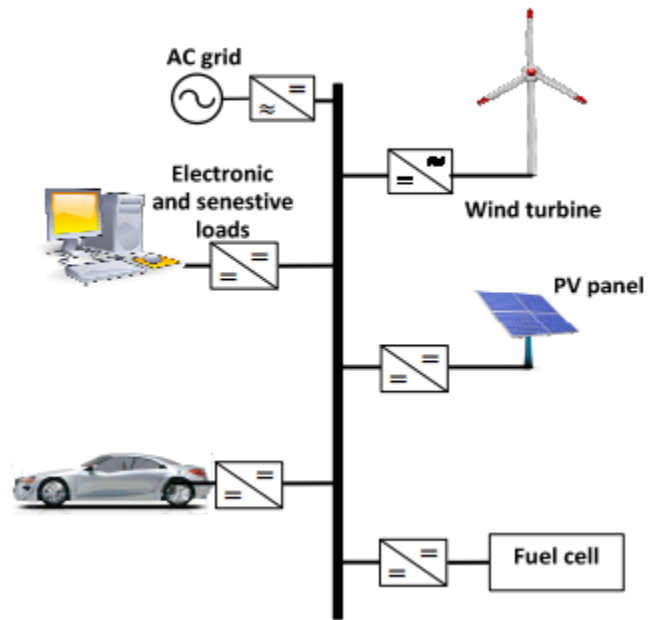


Figure 1.2 DC Microgrid

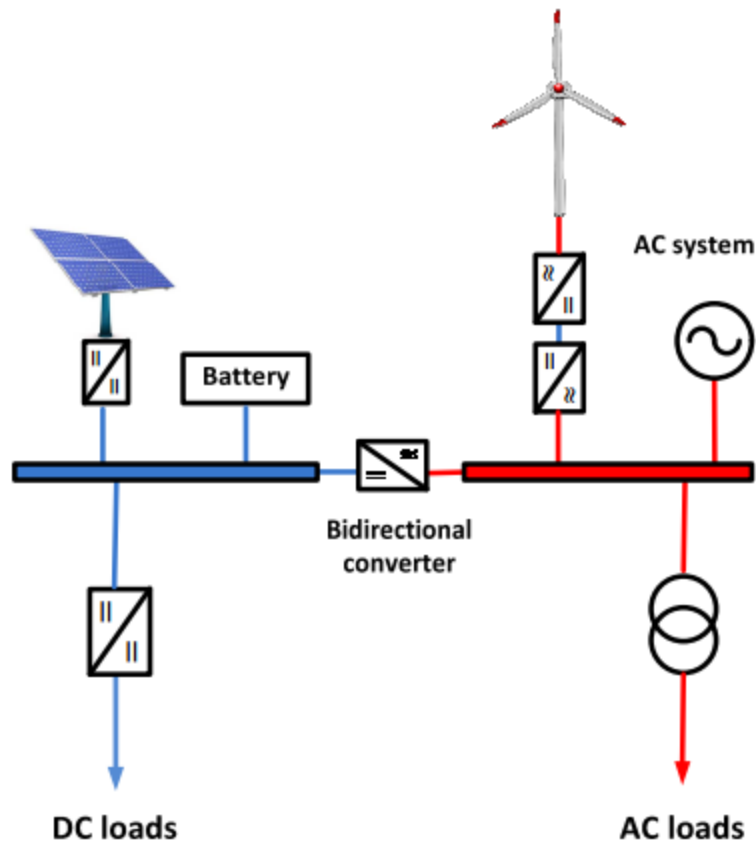


Figure 1.3 Hybrid Microgrid

1.1. Problem Description:

Bidirectional Voltage Source converter (VSC) is an essential component in hybrid microgrids. The challenges in bidirectional converter are; control of power flow in both directions while maintaining stability, efficient transitions between the modes and efficient control of non-linearity.

1.2. Thesis Objectives:

- To Propose the FCS–MPC based control scheme for the bidirectional converter in hybrid microgrid.
- To propose a control strategy, design methodology and mathematical modeling of Active front end (AFE) rectifier using Model Predictive Control (MPC).
- To propose control strategy, design methodology and mathematical modeling of VMPC using Model Predictive Control (MPC) in islanded mode.
- To propose a power control strategy, a design methodology and mathematical modeling of DPMPC using Model Predictive Control (MPC) Grid Connected mode.

1.3. Thesis Organization:

This thesis is systematized as follows:

Chapter 2: This part explains the detail synopsis of control techniques proposed for the Active front End (AFE) rectifier, islanded mode for the hybrid microgrid, grid connected mode of hybrid microgrid. Nonlinear controls and linear control alongside their working standard are examined and toward the finish of section examination among linear and nonlinear control methods are available as table.

Chapter 3: This section investigates working principle, mathematical modeling, structure of proposed controllers Active front end rectifier (AFE), VMPC and DPMPC for hybrid MG and clarify the system parameters.

Chapter 4: The simulations of the proposed techniques are explained in this section and robustness against external variations is validated under different type of tests and different type of loads.

Chapter 5: Conclusion and future work of the proposed work is presented in this section.

Chapter 2

Literature Review

CHAPTER 2. LITERATURE REVIEW

2.1. Classical Control Methods:

2.1.1. Voltage Oriented Control:

Many Topologies and control methods were examined for the improvement of performance and efficiency of Power converter [30], [31]. Traditional control usually depends on the voltage oriented control (VOC) [32], [33]. In stationary α - β Coordinate reactive and active power are divide. It uses PI Controllers with d-q reference rotation by indicating current control loops for power synchronization [34].

In standalone mode, the frequency and voltage of the system is controlled and in grid connected mode, the power controlled and this type of control in which these two parameters are controlled is known as primary control. Power electronics primary control based DGs have many control schemes. Majority of the control methods contain the concept of inner/outer control loop. The current and voltage control comes in category of inner control while droop control comes in the category of outer loop. PID, PR, PI are the controllers that are normally used for these inner and outer control. The complex system is changed in single output loop, single input or the system is linearized in a significant range about the operating point. Thus this linear system does not accommodate more than one input and more than one output or multiple-output and multiple-input also the handling non linearity is not possible. In [35], for controlling DG in microgrid, the adaptive voltage control scheme is propose and has very good instant performance and response. In [36], the method is propose for static synchronous compensator (STATCOM) and is grounded on tuning of PI and it is adaptive in nature. This scheme has the feature to change its control parameters to get the desired response when any disturbances comes. In [37], using the LCL filter, the flow of current is from PEI DG to utility grid. The outer current loop is combined with inner capacitor's loop for the stabilization of system. This scheme has very good results in every situation even

when there is a distortion in capacitor current. The grid current has a THD is in range which is less than 3%. In [38], a scheme is proposed that is based on PI for grid side which has zero steady state error.

2.1.2. Direct Power Control (DPC) and Direct Torque Control (DTC):

Direct Torque control (DTC) and Direct power control (DPC) and are the advanced versions of Hysteresis control [42], [43]. In DTC strategy, control parameters are flux and torque and in DPC, the control parameters are reactive and active powers. To implement this control in digital domain, there is a requirement that the system's switching frequency will be very high for bounding the parameters within the hysteresis bandwidth. The high power applications does not use this scheme because of a drawback of more switching frequency which results in more switching losses. A virtual flux oriented control is explained in which PI controllers are used [44]. The major drawback of PI controllers is their tuning. In addition, direct power control (DPC) [45], [46] was implemented to an AC/DC converter grounded on the principle of direct torque control (DTC) [47], [48], in which PI controller is used.

Direct power control (DPC) is based on look-up table is proposed in order to improve the performance of converter [49], [50]. It uses predefined switching state table in which active and reactive power to perform switching action. Variable switching problem is its drawback which leads to undesirable harmonic contents. To eliminate this issue, fuzzy logic based DPC approach [51] is presented in which predefined switching table is not used. The sampling frequency in fuzzy logic based approach is little bit high but reactive and active powers are good when compared with classical DPC. In grid tied mode, sliding mode [52] nonlinear control is explained to regulate reactive and active power that much depends on variables.

2.1.3. Drawbacks in Linear Controllers:

In voltage source converter's control, the linear controllers gets much matured. There are many drawbacks of linear controllers and many new control strategies are also added in the literature.

One of the major drawback of linear controllers is their tuning. The control parameters in these controllers are tuned on hit and trial basis which consumes lot of our valuable time and very effort. Moreover, external PWM is also required for the generation of pulses. The linear controllers has another drawback that transient response is not dynamic in nature. They also has a drawback that they cannot control multiple parameters at the same time. Taking all the drawbacks in record, it can be easily concluded that linear controllers or PI controllers are not effective in cost, time inefficient and cannot control multiple parameter at the same time.

2.2. Non Linear Control Techniques:

Considering all the above points, world researchers moves towards other techniques that are nonlinear in nature for example Slide Mode Control (SMC), Hysteresis Control, Fuzzy Control, Model Predictive Control etc.

2.2.1. Hysteresis Control:

The referenced and measured currents are compared and the hysteresis upper and lower limits are narrowed and the error is reduced in hysteresis control [39]. It has several advantages and one of them is simple in nature and has also advantage of no modulator required for the signal generation for power electronic devices but its switching frequency changes with variation in the filter parameters, bandwidth of hysteresis and working conditions [40]. It has a major disadvantage that the switching frequency is not controllable. Researchers has done lot of work to eliminate this drawback. This control scheme has switching losses because of it and where high power is needed, this scheme is not used [41].

2.2.2. Sliding Mode Control (SMC):

Slide Mode Control used for both nonlinear and linear systems and it is nonlinear in nature. It is advance control technique [53]. It generates a reference for the load voltage. The controlled variable which is normally load current is bound to follow the predefined path [54]. To accomplish

the steady and powerful response during variety in framework parameters and Load variety, controller arrangement is intentionally changed with reference to structure control act. When contrasted with the linear controller, SMC has ideal execution and great powerful reaction under all instances of activity. But it isn't utilized in viable applications because of the accompanying disservices. Troublesome numerical portrayal and having phenomena of chattering.

2.2.3. Other Non Linear Control Techniques:

The Genetic algorithm, Fuzzy Logic, Artificial Neural Network (ANN), and the mixture of these techniques belongs to intelligent controls and they come in the category of modern nonlinear control methods.

Fuzzy Logic Controller (FLC) works on the criteria of “if-then” instructions. It is non-linear in nature and considered as very good when compared with adaptive controllers [55]. In [56], the voltage and current is controlled based on fuzzy logic controller and it can operate in both islanded and grid tied mode.

Moreover, control methods based on human thinking (human nervous system) are also available and they are known as Artificial Neural network (ANN). Using ANN based controller, the constant switching frequency can be achieved. Neuro-fuzzy logic technique is hybrid in nature and it is the combination of fuzzy and ANN. For the intelligent controller, the information of the operation and behavior of the system is required. There is no need to have an information about the system [57].

2.2.4. Model Predictive Control:

Finally, Predictive control (PC) is a kind of advanced controlled technique and nonlinear and digital in nature. Predictive controllers utilize the framework model to visualize the prospect reactions of the plant. Based on forecast, the ideal control activity is created and connected to the framework, as indicated by the predefined enhancement standard. Between the recently create control techniques, predictive control is one of more wise than typical PID control and successfully utilized in power electronics industry [58]. Despite the fact that during the 1960s, Predictive

control is mined from best control theory. In 1962, Whalen and Zadeh perceived the nearby connection b/w linear programming & optimal control and min. time. Since 1963, moving horizon approach was proposed by propi and it is the base of all predictive control algorithms [59]. PC took attention in compound and procedure Industry in the late 1970s [60, 61]. During the 1980s, MPC also applied in power system which has low switching frequency [62]. Power electronics which has low switching frequency is developed because PC has an additional computational weight for skyline $N > 1$ because of less advancement in chip (MP) innovation. With the progression in MP, Implementation of PC turns out to be simple for higher switching frequency on standard control equipment firm. Because of advancement in DSP's, a wide scope of PC is created which incorporates deadbeat PC, model-based PC (MPC), direction based PC and hysteresis-based PC and an arrangement of PC is appeared in table. 2.1 as proposed in [63, 64].

The concept of optimization in hysteresis predictive control is to bound the controlled parameter inside the given furthest reaches of a region of hysteresis [62]. In direction based predictive control, the factors are compelled to pursue a given direction [65]. In control technique of deadbeat, ideal incitation is the one that calculates the error equivalent to focus in the following examining moment [66].

A progressively adaptable rule is utilized in MPC, communicated as a cost capacity to be limited to choose the ideal activity [60, 67]. MPC is additionally arranged into two classifications:

- FCS-MPC (Finite Control Set MPC).
- CCS-MPC (Continuous Control Set MPC).

CCS-MPC resembles a deadbeat prescient control. CCS-MPC process the continuous signal and need a modulator to create the switching signal for PEDs. Any kind of modulation system can be utilized. Producing constant switching frequency is its main advantage. In any case, FCS-MPC processes the discrete idea of power electronics and it inside creates the switching signals and modulation stage is not required.

For power converters, the developing control strategy is MPC. Fundamentally, MPC is progressive control technique and nonlinear and digital in nature. MPC wipe out the PI controller as well as its modulation stage. MPC pulls in the scientist and industrialists because of its few favorable circumstances, for example, it permits the multivariable framework. It has the quick powerful reaction, straightforward plan, it includes the non-linearity and imperatives of the framework into control law in a simple way [68]. It additionally consolidates settled control circles in just one circle and facilitates to dealing with control deferrals, and power against framework parameter varieties [69, 70]. Also, there is no compelling reason to tune the controller parameters since FCS-MPC is structured utilizing a cost function [71]. Also, FCS-MPC does not require PWM units since it inside produces the gating signals in 0 and 1. Framework limitations legitimately joined the cost function (CF) of the controller to gain the required outcomes. Because of the above-depicted advantages, FCS-MPC a decent device for directing electric power transformation devices. Following reference books [58, 64, 67, 72, and 73] and studies [60, 63, 68, 71, 74, and 75] demonstrates the outcomes and talked about various kinds MPC control for P.E application and their proposed speculations.

In [76], a strategy is proposed that is based on current control is proposed for voltage source inverter. This study utilized the discrete model to foresee the load current. The proposed procedure has a superior dynamic response than traditional linear control. In [77], predictive DPC strategy is proposed for AFE AC-DC. The proposed plan can diminish its switching misfortunes and furthermore control the rectifier power. In [78], an improved model prescient current control had been proposed. The researcher attempts to lessen the spread range by addition of a channel to the factors that are assessed by the cost function. By utilizing this plan, it diminishes the switching losses, so the yield had less harmonics. In [79], creators proposed the predictive power control for battery storage framework and contrasted and PI direct Controller and found that MPC has great outcomes and execution when contrasted with customary PI control. Different BESS with PPC in microgrid Scenario accomplish dynamic outcomes and decrease switching losses and switching frequency. In [80], the voltage improved MPC system for BESS in the independent/standalone mode was proposed. In this work, frequency regulation in the independent/standalone mode of a microgrid is excluded. PI-based MPC procedure and PCC for inward and external control loop

was intended for BESS in [81]. In [82], secondary control of MG is proposed by utilizing MPC knowledge.

Table 2.1 demonstrates the correlation between all control techniques. The old style control plan is full grown and very much perceived in writing and broadly utilizes by PE industry. Rather than that, modern control techniques incorporate new thoughts, complex arithmetic, the casing of reference change, and the regularly required microprocessor. Numerous linear control systems are executed in dq-frame with PID controller and utilizing modulation techniques, for example, PWM and SVM. Table 2.2 shows the comparison table of MPC and linear control is shown in and it shows that MPC is superior to linear controller.

Between control strategies, hysteresis control has the least demanding methodology. There is no need of model and parameters of the system for intelligent control and hysteresis control. Be that as it may, intelligent control strategies requests the former data and view of designers. The limitations are permitted by the SMC and MPC to be included the structure of the controller, yet MPC in such manner is increasingly helpful and basic actualized technique. The response of hysteresis and FCS-MPC has excellent execution under various loading conditions since pulses are produced inside by the procedure. In any case, their switching frequency is variable. In this way, the prerequisite of future application is too full fill the accompanying criteria:

- It should be simplest in digital implementation.
- Performance should be superior to linear control.

FCS-MPC fills these prerequisites, it is a basic and instinctive plan for advanced usage and has dynamic execution during every working condition.

MPC is an advance control technique and it is nonlinear and digital in nature.

Predictive controllers generate future responses using system's mathematical model and the control action is taken based on predefined optimized criteria. It can handle multivariate system and has a rapid dynamic response. System constraints can be easily incorporated into control law. In

addition, nested control loops can be integrated in single loop easily, controlling capability has high delay and when any of the system parameters changes, it shows robustness.

Authors in [83] developed a new algorithm based on model MPC-DPC for AC/DC active rectifiers which can rectifier power and decrease its switching losses. In [84] authors proposed a modified model predictive current control in which they added a filter to the variables to decrease the extent spectrum which are calculated by the CF. The results obtained shows that this method can help to lessen switching losses and overcome harmonics in the scheme. For a battery storage system and compared thus with PI linear control a predictive power control has been developed [85]. Compared to conventional PI control, the MPC was come out to have good results and performance. In [86,87] an strategy proposed for analyzing of predictive current control (PCC) and showed the comparison between the common PCC approach. In [88] the issues like harmonic contents examined briefly that cause due to long prediction horizon in FCS–MPC, but computational complexity is the main complication with long receding horizon. For a four-leg inverter, voltage MPC has been developed which have THD more than 3% in voltage and this is above the legal limit accepted by the some European countries [89].The authors proposed observer-based voltage model predictive control (VMPC) for the applications of UPS which have less system cost but in terms of THD and steady state error, its performance is satisfactory. For VSI with an islanded mode LC filters an implicit MPC has been proposed by the authors in [90] but this tool has helplessness to external uncertainties and parametric variation of the system. Additionally, more computational burden is needed for this system compared to other MPC based techniques. It aides us in measuring the filter and load current instead of estimation and because of the use of sensors it may have increased cost of the system.

Table 2.1 Comparison between Non-linear & linear control technique.

	MPC	DBPC	Intelligent	SMC	Linear	Hysteresis
Switching Frequency	Variable (Controlled)	Fixed	Fixed	Fixed	Fixed	Variable (uncontrolled)
Dynamic Response	Excellent	Good	Good	Good	Average	Excellent
Constraint Inclusion	Possible	No	No	No	No	No
Modulation Stage	Not Required	Required	Required	Required	Required	Not Required
Prior knowledge	No	No	Required	No	No	No
Model & Parameters	Required	Required	No	Required	Required	No
Control Difficulty	Low-Medium	Moderate	Higher	Higher	Moderate	Less

Table 2.2 Comparison between PI & MPC Control.

Description	MPC controller	PI controller
Multivariable	Decoupled	Coupled
Dynamic behavior	Outstanding	Average
Computational Burden	High	Medium
Steady state performance	Better in all 3 frames of reference	Satisfactory in dq Frame
Complexity in Design	Easy	Moderate with SVM
Constraints addition	Easily Possible	Not added
Modulation Scheme	Not Needed	PWM/SVM/SPWM
Switching Frequency	Variable	Fixed
Implementation platform	Only Digital	Both
Type of Controller	Non-Linear	Linear
Design of Controller	Define the Objective function	PI tuning + Modulator design
System Model	Discrete Time model	Linear load model

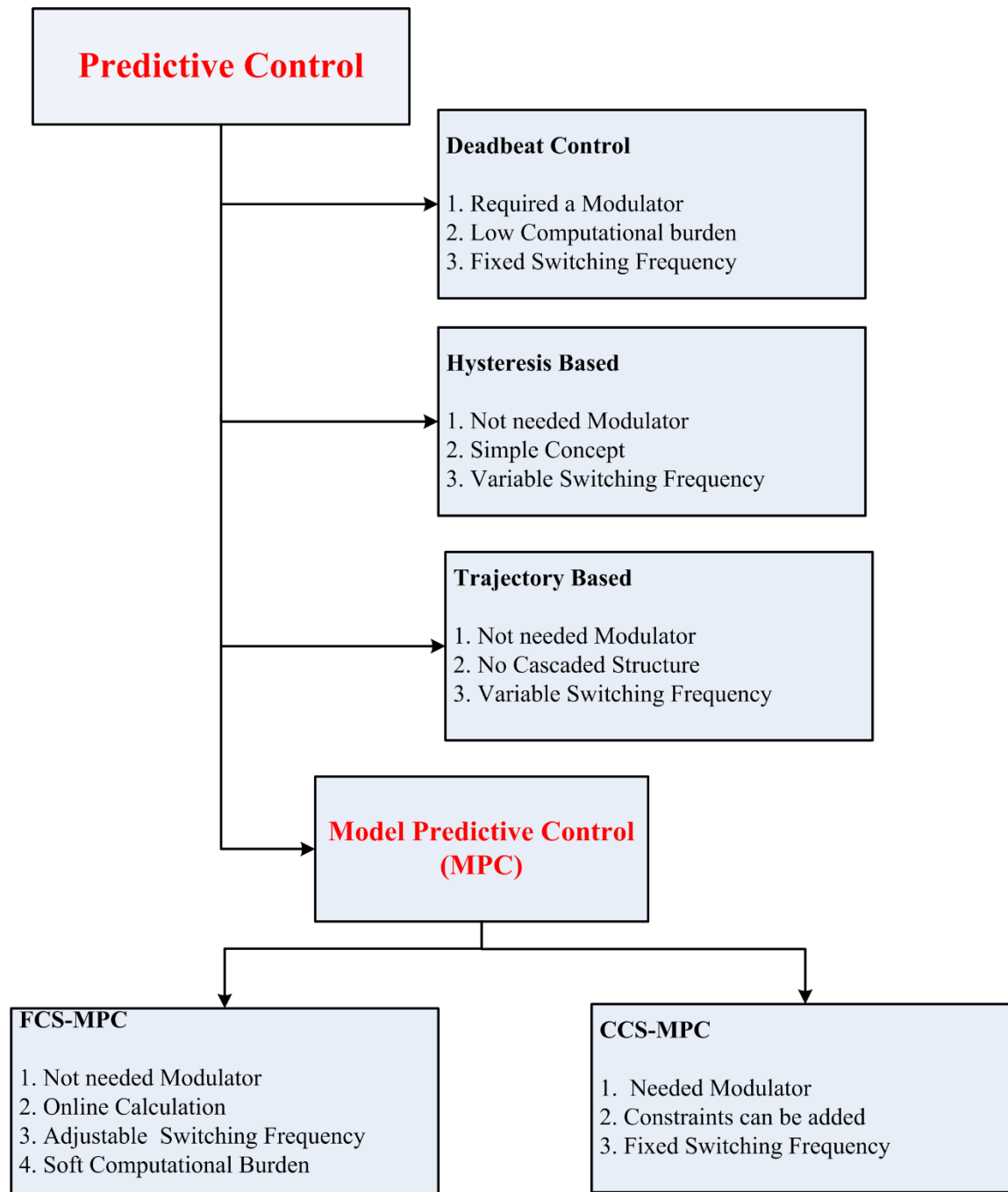


Figure 2.1 Types of Predictive Controllers

Chapter 3

METHODOLOGY

CHAPTER 3. METHODOLOGY

3.1. Mathematical Modeling and Description of the system:

3.1.1. Finite Control Set Model Predictive Control (FCS-MPC):

In FCS-MPC, optimal output is achieved by cost function minimization. The system's model forecast the future value of the parameters for a predefined horizon in time. The basic working of MPC is shown in figure 3.1. This controller has many advantages:

- It is not a complex controller and can be easily implemented.
- It is applicable for various systems.
- It can easily control multivariable system.
- Non linearities can be easily considered in the system model and dead times can be easily rectified.
- Constraints can be simply treated.
- This system is appropriate for the incorporation of changes and augmentations depending on explicit applications.
- Switches gating signals are internally generated.
- outer modulation unit and internal control loops are not needed.
- Modeling of power converter recognizing relation of the

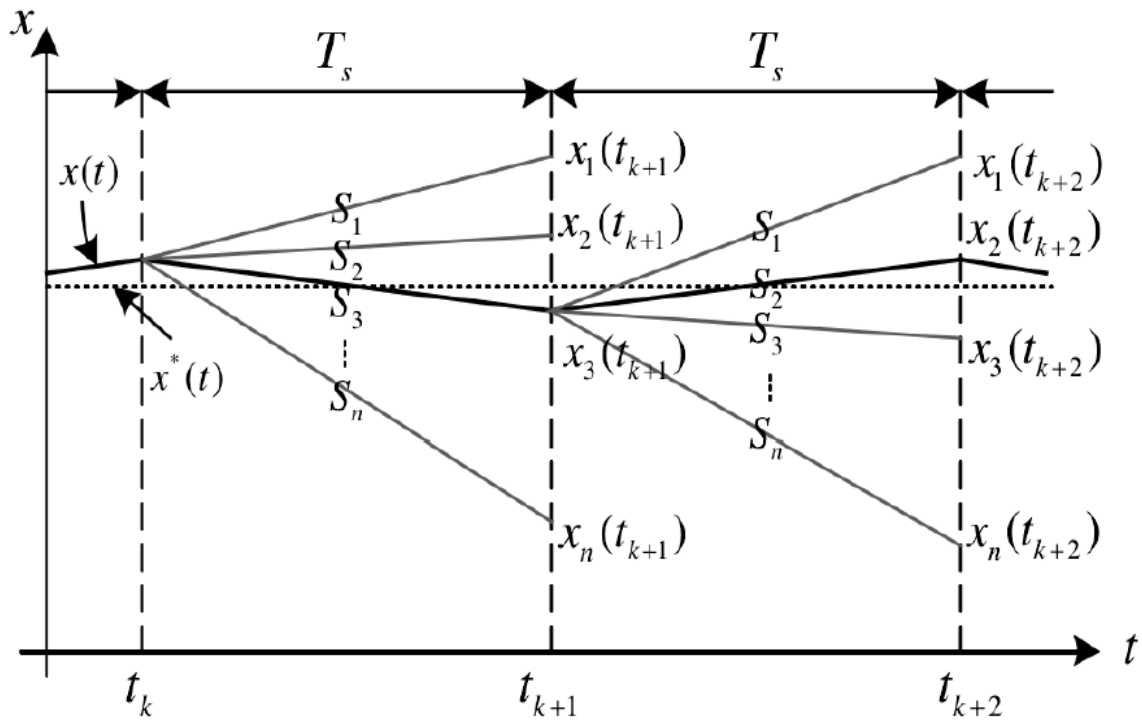


Figure 3.1 Principle of MPC

The fundamental design present in MPC are:

- The future behavior of parameters are forecasted using model until horizon in time.
- The wanted output of the scheme is represented using the cost function.
- The optimal action is taken using cost function minimization.

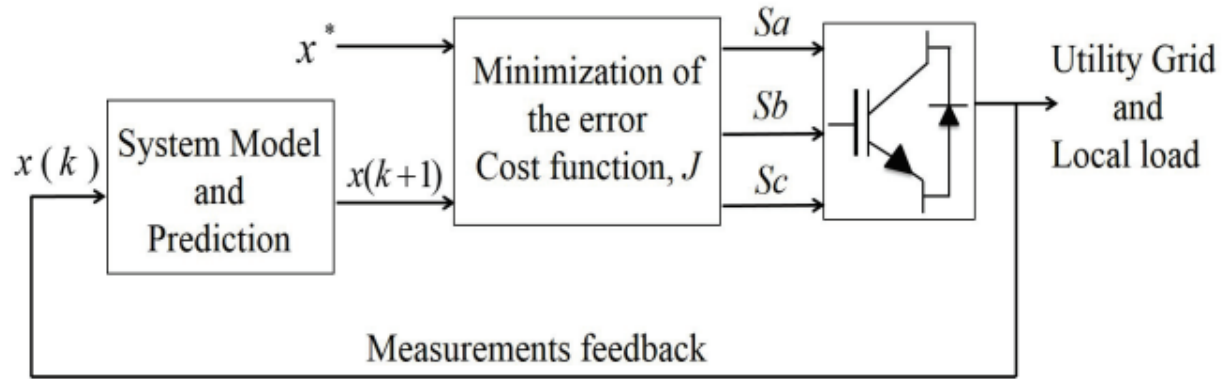


Figure 3.2 Block Diagram of MPC

Figure 3.2 presents the standard control strategy for FCS-MPC that is used for power converters. The future values $x(k+1)$ is predicted using the present values $x(k)$ that are the measurements of output. After this, each possible output of the system is evaluated and by the predefined cost function as shown in equation 3.1 and selects that which has least error between predicted and reference values.

$$J = (x^*(k+1) - x(k+1))^2 \quad (3.1)$$

Where $x(k+1)$ represents the predicted value and $x^*(k+1)$ represents the reference value. After finding optimal output of voltage source converter (VSC), FCS-MPC controller sends proper switching signals to Voltage source converter and the process is repeated continuously at every sampling period. The control scheme can be easily implemented in abc or alpha-beta reference frames and same results achieved in both frames. The computational operations in alpha-beta frames are less as compared to abc frames because we have to control only 2 variables as compared to 3 variables in abc frame. Therefore bidirectional converter is implemented in alpha-beta frames. Clarke's transformation is used to calculate variables in alpha-beta frame.

$$x_{\alpha\beta} = \frac{2}{3} \begin{bmatrix} 1 & -1 & -1 \\ 0 & \frac{\sqrt{3}}{2} & -\frac{\sqrt{3}}{2} \end{bmatrix} \begin{bmatrix} x_a \\ x_b \\ x_c \end{bmatrix} \quad (3.2)$$

$$\vec{x}(t) = x_a(t) + x_b(t) e^{\frac{2\pi}{3}j} + x_c(t) e^{-\frac{2\pi}{3}j} \quad (3.3)$$

$$\overrightarrow{x_{\alpha\beta}}(t) = x_a(t) + jx_b(t) \quad (3.4)$$

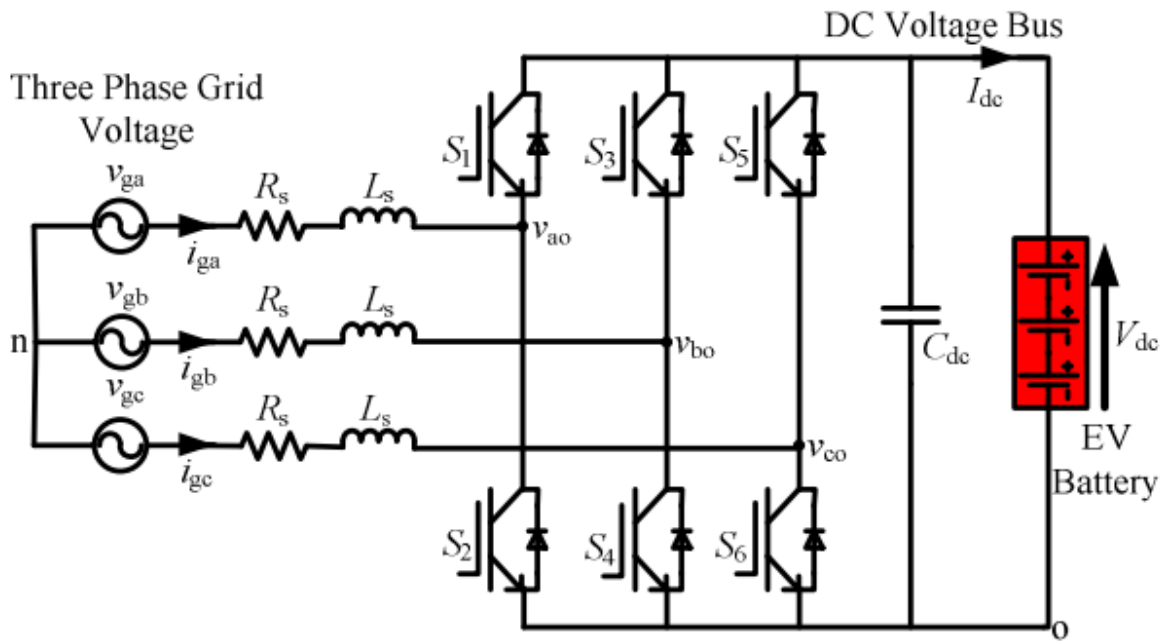


Figure 3.3 Three Phase Bidirectional AC-DC Converter Topology

Bidirectional AC/DC VSC is shown in figure 3.3. It is a 3 phase two-level VSC which contains 3 legs and in every leg there are 2 switches. So, in total it contains six switches as shown in figure 3.3. The gate signals S_a, S_b, S_c controls upper three switches on the basis of SVM and the lower switches are complement of the upper switches. As each leg contains two switches and the possible states are two i-e 0 or 1, so eight switching combinations are possible. Three phase two level converter will have output voltage of V_t from one of the eight vectors, V_n . Among these eight vectors, two vectors results zero, so they are called zero vectors and other six vectors are expressed as:

$$V_n = \frac{2}{3} v_{dc} e^{j(n-1)\frac{\pi}{3}} \quad n = (1, \dots, 6) \quad (3.5)$$

Table 3.1 Voltage Space vector of Bidirectional AC-DC Bidirectional Converter

Switching States			Voltage space vector
S_a	S_b	S_c	\vec{v}_{conv}
0	0	0	$\vec{v}_1 = 0$
0	0	1	$\vec{v}_2 = -(1/3)V_{dc} - j(\sqrt{3}/3)V_{dc}$
0	1	0	$\vec{v}_3 = -(1/3)V_{dc} + j(\sqrt{3}/3)V_{dc}$
0	1	1	$\vec{v}_4 = -(2/3)V_{dc}$
1	0	0	$\vec{v}_5 = (2/3)V_{dc}$
1	0	1	$\vec{v}_6 = (1/3)V_{dc} - j(\sqrt{3}/3)V_{dc}$
1	1	0	$\vec{v}_7 = (1/3)V_{dc} + j(\sqrt{3}/3)V_{dc}$
1	1	1	$\vec{v}_8 = 0$

Table 3.2 Switching State Definition

Switching State	Leg X			Leg Y			Leg Z		
	S'_1	S'_4	V_{AN}	S'_3	S'_6	V_{BN}	S'_5	S'_2	V_{CN}
P	ON	OFF	V_d	ON	OFF	V_d	ON	OFF	V_d
O	OFF	ON	Zero	OFF	ON	Zero	OFF	ON	Zero

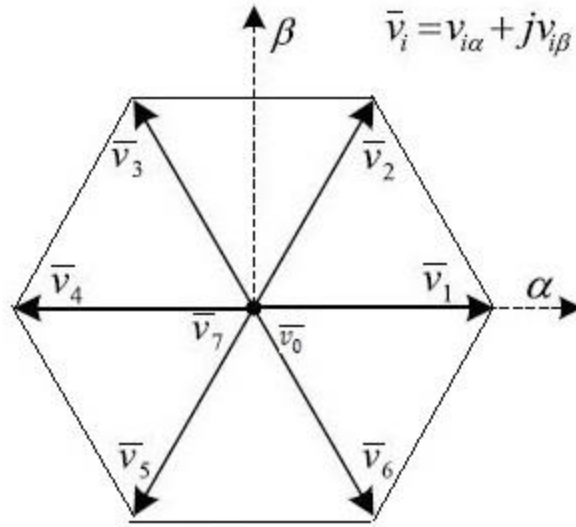


Figure 3.4 Space Vector Modulation

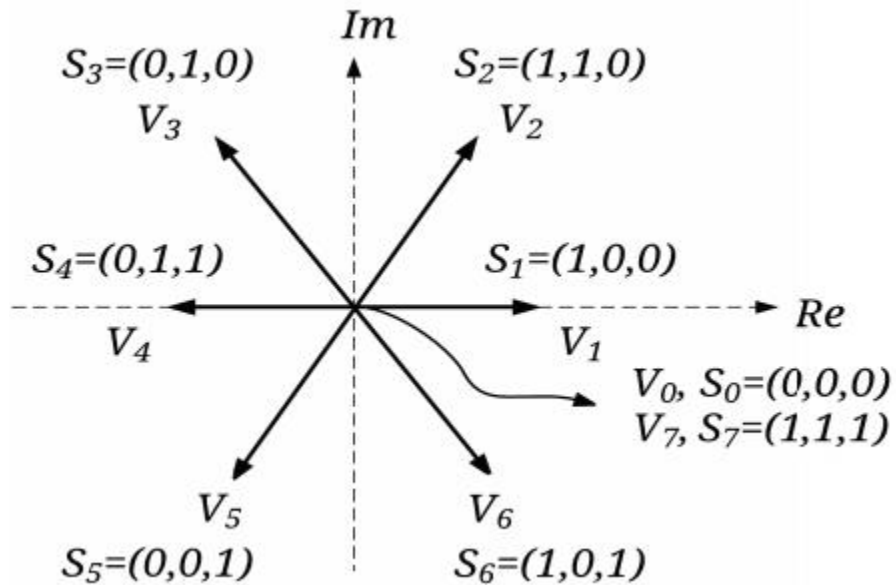


Figure 3.5 Voltage Vectors Generated by VSC

Where V_n represents the output voltage vectors of VSC. V_{dc} shows the DC side voltage. The six different combinations of voltage vectors (V_1 to V_6) that are obtained from voltage space vectors

equation. The zero output voltage vectors are V_0 and V_7 . The switch mix ($S_a S_b S_c$) for these eight conceivable yield voltages (V_0, V_1, \dots, V_7) are the accompanying: 000, 100, 110, 010, 011, 001, 101, and 111, separately (where 1/0 implies the switch is ON/OFF) The voltage space vectors, which are formed by the three-stage two-level Converter are shown in table 3.1.

3.1.2. Control of an Active Front End Rectifier:

The converters that are mostly used in power electronics are rectifiers. They can convert AC current to DC current and have many applications for small as well as large power applications.

3.6(a) shows the simplest diode rectifier topology which controls DC voltage and the diodes commutation is done using AC voltage. It operates at low frequency and it is also called as line-commutated rectifier. It is easy in nature very low cost as well. Three phase diode rectifier has some disadvantages and limitations which are:

- Control of power flow is not possible.
- In the input side when capacitive load is connected, harmonics are generated in the input current. Output voltage is filtered using this capacitor.
- Regeneration of power is not possible.

Figure 3.6(b) shows the thyristor rectifier which allows the power flow control by changing the gate pulses angle (α). By using angle (α), power of the load can be controlled [91] and mean value of load voltage can also be changed [91]. The diode rectifiers and thyristor rectifiers have approximately same advantages and disadvantages. It has one additional disadvantage that by increasing the value of α , the phase displacement among AC source voltage and input current get changed, thus reactive power is increased. The thyristor rectifier has an advantage of regenerating power from DC load to source when operating angle is greater than 90.

3.6(c) shows the third important topology which consist of power transistors with antiparallel diodes. This topology operates at more switching frequency. It is called as active front end (AFE) rectifier. It eliminates all the issues that were in thyristor and diode rectifiers [92]. Main characteristics of this topology are:

- Controlled DC voltage.
- Reduced harmonics.
- It operates with high power factor.
- Full regenerative operation.

This topology has a negative feature of high cost compare to diode and thyristor rectifiers.

The control schemes for AFE rectifier are DPC and VOC [93].

In VOC, input currents are align with reference to the line voltage vector and regulation of reactive and active power is controlled by controlling currents [94]. In this scheme, reactive power proportional to i_q and active power proportional to i_d . For unity power factor current i_q reference is fixed to 0. The PI controller controls dc voltage and the reference current is generated which then controls the active power. It has very good static and dynamic behavior but the quality depends on control strategies.

In DPC, currents are measured after which reactive and active powers are approximated. It is regulated directly with switching table and hysteresis controllers similar to the DTC [95,96].

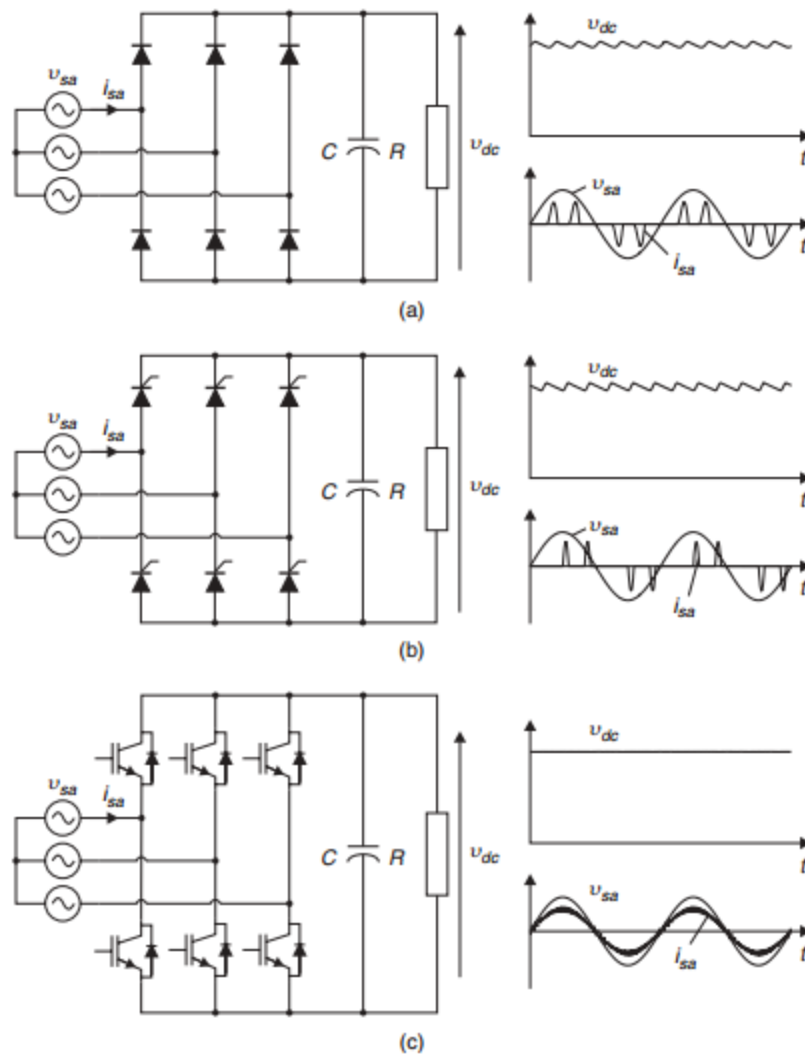


Figure 3.6 Rectifier Topologies

3.1.2.1. Rectifier Model:

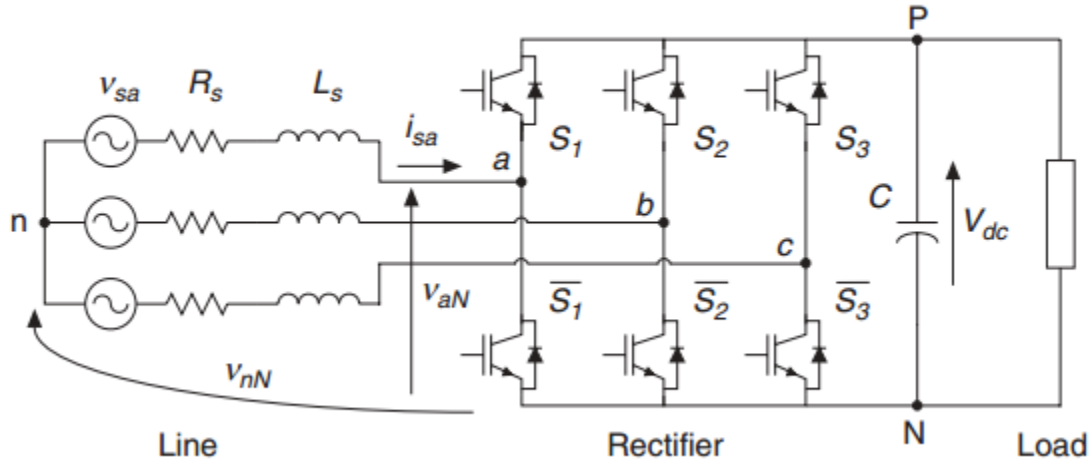


Figure 3.7 AFE Model

Figure 3.7 represents the model of AFE rectifier. It is fully controlled and consist of power transistors attached to 3 phase source vs filter resistance R_s and inductances L_s . The equations 3.6, 3.7, 3.8 are the equations of each phase:

$$v_{sa} = L_s \frac{di_{sa}}{dt} + R_s i_{sa} + v_{aN} - v_{nN} \quad (3.6)$$

$$v_{sb} = L_s \frac{di_{sa}}{dt} + R_s i_{sa} + v_{aN} - v_{nN} \quad (3.7)$$

$$v_{sc} = L_s \frac{di_{sa}}{dt} + R_s i_{sa} + v_{aN} - v_{nN} \quad (3.8)$$

Space vector for the grid voltage is

$$v_s = \frac{2}{3}(v_{sa} + av_{sb} + a^2v_{sc}) \quad (3.9)$$

Where $a = e^{\frac{j2\pi}{3}}$ and grid dynamic currents can be obtained by substituting 3.6 to 3.8 into 3.9

$$v_s = L_s \frac{d}{dt} (i_{sa} + ai_{sb} + a^2i_{sc}) + Rs \frac{2}{3} (i_{sa} + ai_{sb} + a^2i_{sc}) + \frac{2}{3} (v_{aN} + av_{bN} + a^2v_{cN}) - \frac{2}{3} (v_{nN} + av_{nN} + a^2v_{nN}) \quad (3.10)$$

Equation 3.10 has a last term equal to zero

$$\frac{2}{3} (v_{nN} + av_{nN} + a^2v_{nN}) = v_{nN} \frac{2}{3} (1 + a + a^2) = 0 \quad (3.11)$$

Following grid current and AFE's generated voltage vectors are used to simplify the input current dynamic equations (3.10)

$$i_s = \frac{2}{3} (i_{sa} + ai_{sb} + a^2i_{sc}) \quad (3.12)$$

$$v_{afe} = \frac{2}{3} (v_{aN} + av_{bN} + a^2v_{cN}) \quad (3.13)$$

v_{afe} is determined by DC link voltage and Switching state vector and expressed as:

$$v_{afe} = s_{afe} v_{dc} \quad (3.14)$$

V_{dc} shows the DC link voltage s_{afe} shows switching state vector and it is defined as defined as:

$$s_{afe} = \frac{2}{3}(s_1 + as_2 + a^2s_3) \quad (3.15)$$

Where $s_x(s_1, s_2, s_3)$ are the rectifier's switching states and it has value of 0 if s_x is off and it is 1 if s_x is 1 ($x = 1, 2, 3$).

In stationary $\alpha\beta$, the input dynamic equations are represented as:

$$L_s \frac{di_s}{dt} = v_s - v_{afe} - R_s i_s \quad (3.16)$$

Where v_s shows the supply voltage, v_{afe} shows the voltage produced by converter i_s shows the input current.

3.1.2.2. Discrete Time Model:

The current is predicted by the following discrete time equation:

$$i_s(k+1) = \left(1 - \frac{R_s T_s}{L_s}\right) i_s(k) + \frac{T_s}{L_s} [v_s(k) - v_{afe}(k)] \quad (3.17)$$

Where T_s shows the sampling time. This equation is obtained by discretizing equation 3.16. The discretization is done by taking the one sampling period and derivative is approximated as difference. The instantaneous reactive and active power are predicted from the following eq:

$$P_{in}(k+1) = Re\{v_s(k+1)\bar{i}_s(k+1)\} = v_{s\alpha}i_{s\alpha} + v_{s\beta}i_{s\beta} \quad (3.18)$$

$$Q_{in}(k + 1) = I_m \{v_s(k + 1)\bar{i}_s(k + 1)\} = v_{s\alpha}i_{s\alpha} - v_{s\beta}i_{s\beta} \quad (3.19)$$

Where $i_s(k + 1)$ shows predicted input current vector, $\bar{i}_s(k + 1)$ is the complex conjugate of the input current vector, v_{afe} shows the rectifier's generated voltage vector.

3.1.2.3. Predictive Power Control:

The behavior of input reactive and active power at the input of converter can be predicted using this model and knowing the knowledge of instantaneous power theory [97]. After this, If the cost function is correctly described the flow of power among the grid and the converter can be easily controlled [98]. At the central time instant, the converter's switching state is constant for the complete sampling time. The switching states selection is done by the cost minimization criteria at each sampling interval. The state that will generate less error will be selected. This strategy does not need any external modulators nor and internal control loops. The reactive and active powers are controlled by simply forcing currents.

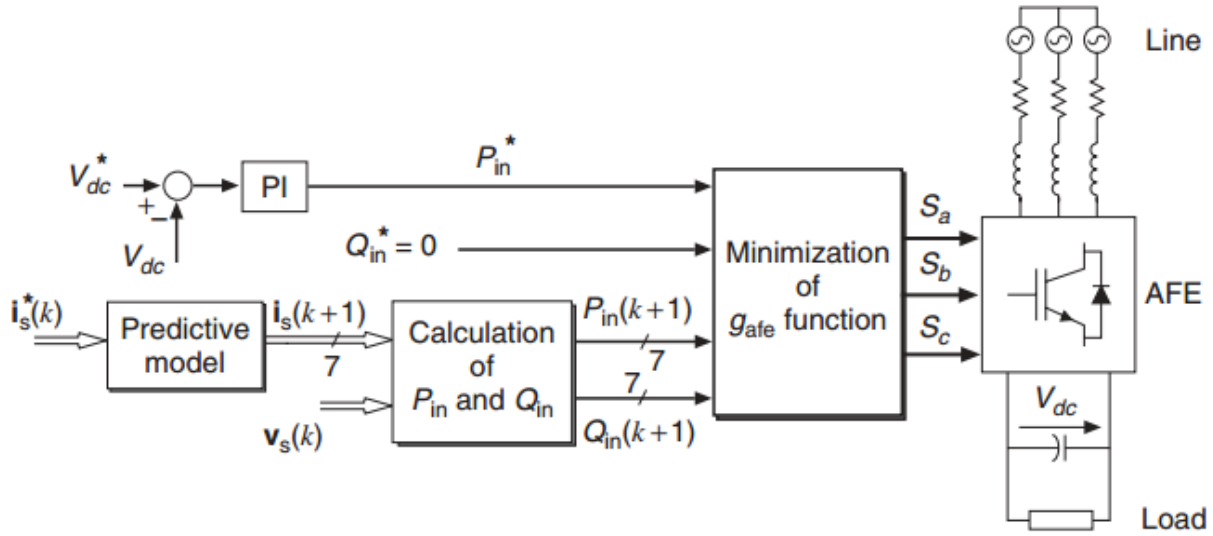


Figure 3.8 Predictive Power Control

3.1.2.4. Cost function and control scheme:

Figure 3.8 shows the block diagram of control strategy. In this strategy, voltage vector $V_{afe}(k)$ generated by AFE is used to calculate future value the input currents $i_s(k+1)$ using input current $i_s(k)$. Total seven possible values of future input currents $i_s(k+1)$ are predicted for every voltage vector v_{afe} . After this, future input reactive power $Q_{in}(k+1)$ and active power $P_{in}(k+1)$ are calculated using predictive currents using eq (3.18) and (3.19). Then cost function g_{afe} is evaluated on the basis of these predictive reactive power $Q_{in}(k+1)$ and active power $P_{in}(k+1)$. At the end, desired behavior is achieved by the CF g_{afe} i-e reactive power error and active power errors are minimized by comparing their values with the reference values by the eq:

$$g_{afe} = |Q_{in}^* - Q_{in}(k+1)| + |P_{in}^* - P_{in}(k+1)| \quad (3.20)$$

DC link voltage are regulated through PI controller. For stabilizing the DC link output voltage and to eliminate error in the desired output, the PI controller gives output power. This generates the

reference for the active power. Reactive power reference value is fixed to zero. However we can also set the reactive power other than zero in some applications. Voltage vectors $v_{afe}(k)$ will generate different values of cost function and for every next interval, the voltage vector $v_{afe}(k)$ through which the cost function g_{afe} is minimized will be selected.

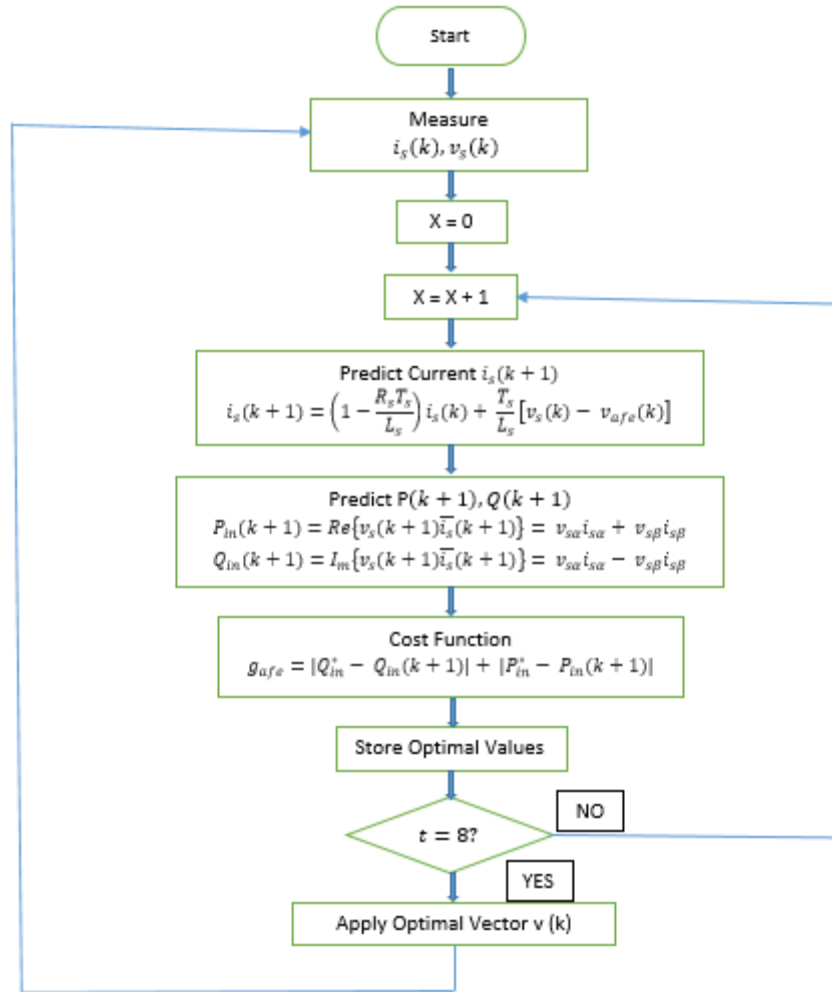


Figure 3.9 Active Front End (AFE) Rectifier Flowchart

3.2. Voltage Model Predictive Control in Islanded Mode:

When microgrid and utility are disconnected from each other then islanding occurs. In this mode frequency (Hz) and voltage (V) of the microgrid is not fixed. It has to be controlled because we lost our reference. So controller control the frequency (Hz) and voltage (V) of the microgrid. The mathematical model of the system is described as:

$$i_l = i_o \quad (3.21)$$

$$i_c = i_f - i_o \quad (3.22)$$

$$V_c = V_{pc} \quad (3.23)$$

$$v_t = v_{pc} + v_f + i_f R_f \quad (3.24)$$

Where,

$i_l = \text{load current}$

$i_c = \text{filter capacitor Current}$

$i_f = \text{filter inductor Current}$

$i_o = \text{load Current}$

$v_t = \text{Voltage source converter voltage}$

$v_{pc} = \text{Voltage at the point of common coupling}$

$v_f = \text{Inductor Voltage}$

By using dynamical equations of the filter capacitor voltage and inductor current, the continuous state space model can be determined easily and it can be expressed as:

$$i_c = i_f - i_0 \quad (3.25)$$

$$C_f \frac{dV_{pc}}{dt} = i_f - i_0 \quad (3.26)$$

$$\frac{dV_{pc}}{dt} = \frac{1}{C_f} (i_f - i_0) \quad (3.27)$$

$$v_t = v_{PC} + v_f + i_f R_f \quad (3.28)$$

$$L_f \frac{di_f}{dt} = v_t - v_{PC} - i_f R_f \quad (3.29)$$

$$\frac{di_f}{dt} = \frac{1}{L_f} (v_t - v_{PC} - i_f R_f) \quad (3.30)$$

The continuous state space model can be determined by the equations 3.27 and 3.30:

$$\frac{dx}{dt} = Ax + B_1 v_t + B_2 i_0 \quad (3.31)$$

$$x = \begin{bmatrix} i_f \\ v_{pc} \end{bmatrix} \quad (3.32)$$

$$A = \begin{bmatrix} -R_f & -1 \\ \frac{L_f}{C_f} & 0 \end{bmatrix} \quad (3.33)$$

$$B_1 = \begin{bmatrix} 1 \\ \frac{1}{L_f} \\ 0 \end{bmatrix} \quad (3.34)$$

$$B_2 = \begin{bmatrix} 0 \\ 1 \\ -\frac{1}{c_f} \end{bmatrix} \quad (3.35)$$

$$\frac{dx}{dt} = \begin{bmatrix} \frac{-R_f}{L_f} & \frac{-1}{C_f} \\ \frac{1}{C_f} & 0 \end{bmatrix} \begin{bmatrix} i_f \\ v_{pc} \end{bmatrix} + \begin{bmatrix} \frac{1}{L_f} \\ 0 \end{bmatrix} v_t + \begin{bmatrix} 0 \\ -\frac{1}{c_f} \end{bmatrix} i_0 \quad (3.36)$$

The system's discrete time model can be found by the method of Euler forward method of approximation.

$$\frac{dx}{dt} = \frac{x(t_k + 1)' - x(t_k)}{T_s} \quad (3.37)$$

$$(t_k + 1)' = A_d x(t_k) + B_{1d}V_t(t_k) + B_{2d}i_0(t_k) \quad (3.38)$$

$$A_d = e^{AT_s} \quad (3.39)$$

$$B_{1d} = \int_0^{T_s} e^{A\tau} B_1 d\tau \quad (3.40)$$

$$B_{2d} = \int_0^{T_s} e^{A\tau} B_2 d\tau \quad (3.41)$$

Exponential matrix can be approximated as equation 3.42 if the sampling time is very small.

$$e^{AT_s} \approx 1 + AT_s \quad (3.42)$$

Now for the next sampling instant (k+1), the imaginary and real parts (i.e., $\alpha\beta$) of the filter capacitor voltage and filter inductor current are found using the measured discrete values of $i_f(k), i_o(k), v_{pc}(k)$.

$$v_{c,\alpha}(t_k + 1) = v_{pc,\alpha}(t_k) + \frac{T_s}{C_f} \left(i_{f,\alpha}(t_k) - i_{0,\alpha}(t_k) \right) \quad (3.43)$$

$$v_{c,\beta}(t_k + 1) = v_{pc,\beta}(t_k) + \frac{T_s}{C_f} \left(i_{f,\beta}(t_k) - i_{0,\beta}(t_k) \right) \quad (3.44)$$

$$i_{f,\alpha}(t_k + 1) = i_{f,\alpha} + \frac{T_s}{L_f} \left(v_{t,\alpha}(t_k) - v_{pc,\alpha}(t_k) \right) - \frac{R_f T_s}{L_f} i_{f,\alpha}(t_k) \quad (3.45)$$

$$i_{f,\beta}(t_k + 1) = i_{f,\beta} + \frac{T_s}{L_f} \left(v_{t,\beta}(t_k) - v_{pc,\beta}(t_k) \right) - \frac{R_f T_s}{L_f} i_{f,\beta}(t_k) \quad (3.46)$$

The second step sampling instant (k+2) is predicted for the optimization of the capacitor output value to allow the cost function to find for each voltage vector. Equations of capacitor's voltage are found and expressed as:

$$v_{c,\alpha}(t_k + 2) = v_{pc,\alpha}(t_k + 1) + \frac{T_s}{C_f} \left(i_{f,\alpha}(t_k + 1) - i_{0,\alpha}(t_k) \right) \quad (3.47)$$

$$v_{c,\beta}(t_k + 2) = v_{pc,\beta}(t_k + 1) + \frac{T_s}{C_f} \left(i_{f,\beta}(t_k + 1) - i_{0,\beta}(t_k) \right) \quad (3.48)$$

It is assumed that the variation in load current will be very small if the sampling interval (T_s) is small for the whole prediction time.

$$i_{0,\alpha}(t_k + 1) = i_{0,\alpha}(t_k) \quad (3.49)$$

$$i_{0,\beta}(t_k + 1) = i_{0,\beta}(t_k) \quad (3.50)$$

The cost function will be:

$$g_v = (v_{c,\alpha}^*(t_k + 2) - v_{c,\alpha}(t_k + 2))^2 + (v_{c,\beta}^*(t_k + 2) - v_{c,\beta}(t_k + 2))^2 \quad (3.51)$$

Where referenced $\alpha\beta$ values are represented by $v_{c,\alpha}^*(t_k + 2)$, $v_{c,\beta}^*(t_k + 2)$ and the predicted values are represented by $v_{c,\alpha}(t_k + 2)$, $v_{c,\beta}(t_k + 2)$

Finally the Voltage Model predictive Control (VMPC) flow chart is shown in the figure 3.10.

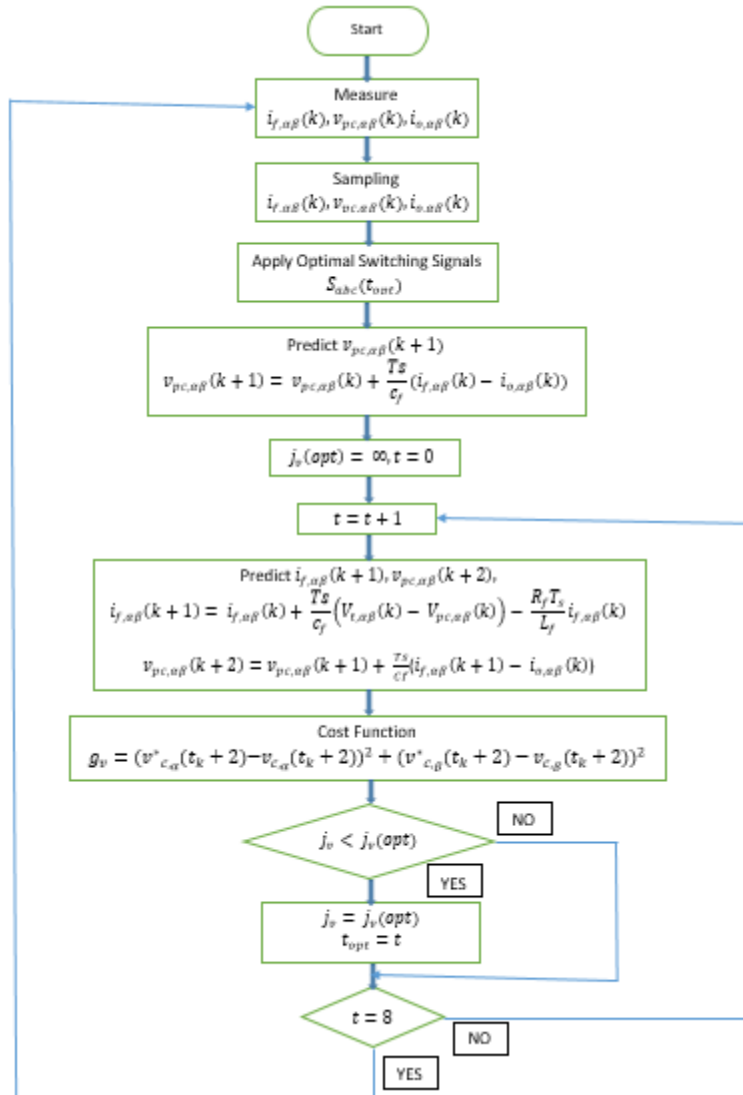


Figure 3.10 VMPC Flowchart

3.3. Direct Power Model Predicted Control in Grid Connected Mode:

When the utility grid is connected with the microgrid, it is in the grid connected mode. The utility grid will generate reference of frequency and voltage. The power can be controlled between voltage source converter (VSC) and microgrid. System's mathematical model is:

$$i_l = i_0 - i_g \quad (3.52)$$

$$i_c = i_f - i_0 \quad (3.53)$$

$$v_t = v_{pc} + v_f + i_f R_f \quad (3.54)$$

$i_g =$ current flowing to the utility grid.

The exchange of reactive and active powers among the grid and between the VSC and PCC can be obtained by:

$$\begin{bmatrix} P \\ Q \end{bmatrix} = \frac{3}{2} \begin{bmatrix} v_{pc,\alpha} & v_{pc,\beta} \\ v_{pc,\beta} & -v_{pc,\alpha} \end{bmatrix} \begin{bmatrix} i_{f\alpha} \\ i_{f\beta} \end{bmatrix} \quad (3.55)$$

$$P = \frac{3}{2} (v_{pc,\alpha} i_{f,\alpha} + v_{pc,\beta} i_{f,\beta}) \quad (3.56)$$

$$Q = \frac{3}{2} (v_{pc,\beta} i_{f,\alpha} - v_{pc,\alpha} i_{f,\beta}) \quad (3.57)$$

When Q and P are differentiated w.r.t time, the output will be state space (continuous time) model of the scheme. It is expressed as:

$$\frac{dP}{dt} = \frac{3}{2} \left(\frac{dv_{pc,\alpha}}{dt} i_{f,\alpha} + v_{pc,\alpha} \frac{di_{f,\alpha}}{dt} + \frac{dv_{pc,\beta}}{dt} i_{f,\beta} + \frac{di_{f,\beta}}{dt} v_{pc,\beta} \right) \quad (3.58)$$

$$\frac{dQ}{dt} = \frac{3}{2} \left(\frac{dv_{pc,\beta}}{dt} i_{f,\alpha} + v_{pc,\beta} \frac{di_{f,\alpha}}{dt} - \frac{dv_{pc,\alpha}}{dt} i_{f,\beta} - v_{pc,\alpha} \frac{di_{f,\beta}}{dt} \right) \quad (3.59)$$

$\frac{dv_{pc,\alpha}}{dt}$, $\frac{di_{f,\alpha}}{dt}$, $\frac{dv_{pc,\beta}}{dt}$, and $\frac{di_{f,\beta}}{dt}$ are determined to find the continuous time state space model. The system is consider balanced sinusoidal, V_{pc} can be fined by:

$$v_{pc} = v_{pc,\alpha} + i v_{pc,\beta} \approx |v_{pc}| e^{-i\omega t} \quad (3.60)$$

After taking explicit derivate of equation a, we get:

$$\frac{dv_{pc,\alpha}}{dt} = \omega v_{pc,\beta} \quad (3.61)$$

$$\frac{dv_{pc,\beta}}{dt} = -\omega v_{pc,\alpha} \quad (3.62)$$

Where angular frequency at PCC voltage is measured in ω and it is measured in rad/sec. It can be found by PLL. The equation 3.54 is use to determine real and imaginary dynamical equations of current.

$$\frac{di_{f,\alpha}}{dt} = \frac{1}{L_f} (v_{t\alpha} - v_{pc,\alpha} - i_{f,\alpha} R_f) \quad (3.63)$$

$$\frac{di_{f,\alpha\beta}}{dt} = \frac{1}{L_f} (v_{t\beta} - v_{pc,\beta} - i_{f,\beta} R_f) \quad (3.64)$$

$$\frac{dx}{dt} = A_g x + \frac{3}{2L_f} B_{1g} v_t - \frac{3}{2L_f} B_{2g} v_{pc} \quad (3.65)$$

$$x = \begin{bmatrix} P \\ Q \end{bmatrix} \quad (3.66)$$

$$A_g = \begin{bmatrix} \frac{-R_f}{L_f} & -\omega \\ \omega & \frac{-R_f}{L_f} \end{bmatrix} \quad (3.67)$$

$$B_{1g} = \begin{bmatrix} v_{pc,\alpha} & v_{pc,\beta} \\ v_{pc,\beta} & -v_{pc,\alpha} \end{bmatrix} \quad (3.68)$$

$$B_{2g} = \begin{bmatrix} v_{pc,\alpha} & v_{pc,\beta} \\ 0 & 0 \end{bmatrix} \quad (3.69)$$

$$\frac{dx}{dt} = \frac{x(t_k + 1)' - x(t_k)}{T_s} \quad (3.70)$$

$$x(t_k + 1)' = A_{g1} x(t_k) + B_{g1} V_t(t_k) + B_{g2} i_0(t_k) \quad (3.71)$$

$$A_{g1} = e^{A_g T_s} \quad (3.72)$$

$$B_{g1} = \int_0^{T_s} e^{A_g \tau} B_{1g} d\tau \quad (3.73)$$

$$B_{g2} = \int_0^{T_s} e^{A_g \tau} B_{2g} d\tau \quad (3.74)$$

Exponential function can be approximated if sampling time is very small.

$$e^{A_g T_s} \approx 1 + A_g T_s \quad (3.75)$$

The above equations are used to sing reactive and active power and it is expressed as:

$$\begin{aligned} P(t_k + 1)' = P(t_k) & \quad (3.76) \\ & + T_s \left[\frac{-R_f}{L_f} P(t_k) - \omega Q(t_k) \right. \\ & + \frac{3}{2L_f} \left(v_{pc,\alpha}(t_k) v_{t_\alpha}(t_k) + v_{pc,\beta}(t_k) v_{t_\beta}(t_k) \right) - \frac{3}{2L_f} (v_{pc,\alpha}^2(t_k) \\ & \left. + v_{pc,\beta}^2(t_k)) \right] \end{aligned}$$

$$\begin{aligned} Q(t_k + 1)' = Q(t_k) & \quad (3.77) \\ & + T_s \left[\frac{-R_f}{L_f} Q(t_k) + \omega P(t_k) \right. \\ & \left. + \frac{3}{2L_f} \left(v_{pc,\alpha}(t_k) v_{t_\alpha}(t_k) + v_{pc,\beta}(t_k) v_{t_\beta}(t_k) \right) \right] \end{aligned}$$

Finally the cost function will be represented as:

$$g_{DPMPC} = (P^*(t_k + 1)' - P(t_k + 1)')^2 + (Q^*(t_k + 1)' - Q(t_k + 1)')^2 \quad (3.78)$$

Where $P^*(t_k + 1)'$ represents active power reference value.

$Q^*(t_k + 1)'$ Represents reactive power reference value.

$P(t_k + 1)'$ Represents predicted value of active power.

$Q(t_k + 1)'$ Represents predicted value of reactive power.

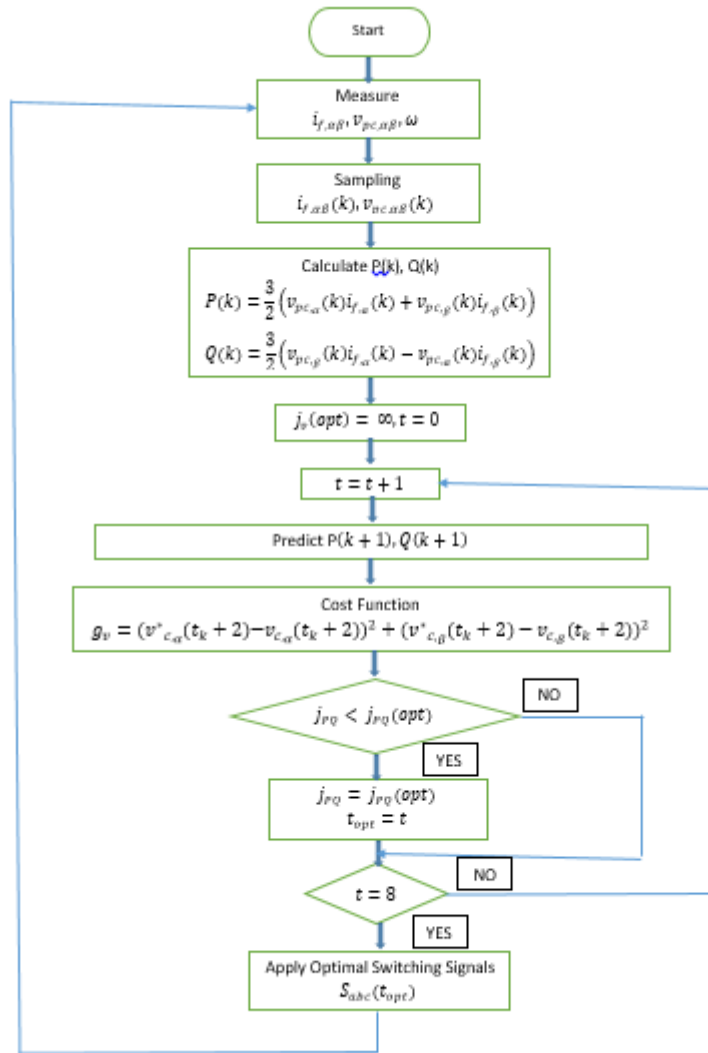


Figure 3.11 DPMPFC Flowchart

Chapter 4

Results

CHAPTER 4. RESULTS

Performance of the Bidirectional Voltage Source Converter (VSC) based on MPC controller for hybrid microgrid is validated by considering different test cases and MATLAB/SIMULINK is used for the responses and analysis and effectiveness of MPC is confirmed under different test conditions.

Different cases are:

1. Bidirectional VSC as Active Front End (AFE) Rectifier
 - 1.1. Regulation of DC link Voltage.
 - 1.2. Step Change in DC link Voltage.
 - 1.3. Step Change in Load.
 - 1.4. Regulation of power/Step Change in power.
2. Bidirectional VSC as Voltage Source Inverter (Grid Connected Mode)
 - 2.1. Regulation of Power/Step Change in power.
 - 2.2. Unbalanced Linear Load.
3. Bidirectional VSC as Voltage Source Inverter (Islanded Mode)
 - 3.1. Regulation of voltage and frequency.
 - 3.2. Step Change in linear Load.
 - 3.3. Non Linear Load.
4. Transitions Between the modes of microgrid.

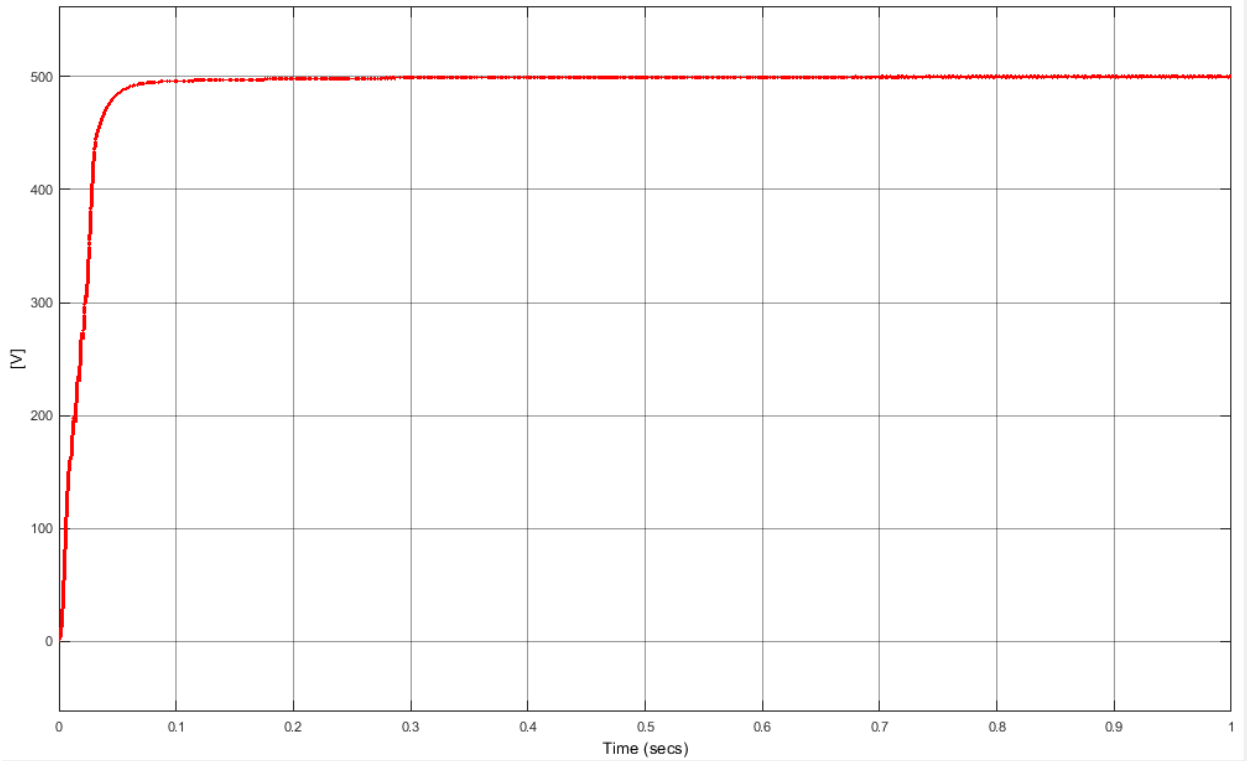
Table 4.1 Parameters for the simulations

Parameters	Symbols	Values
Sampling Frequency	T_s	$33\mu s$
Grid Voltage	V_g	$110V_{rms}$
Grid Frequency	f	$50Hz$
Filter capacitance	C_f	$250\mu F$
Filter resistance	R_f	$0.1ohm$
Filter Inductance	L_f	$10mh$
DC Bus Voltage	V_{dc}	$500V$
DC link Capacitor	C	$2000\mu F$

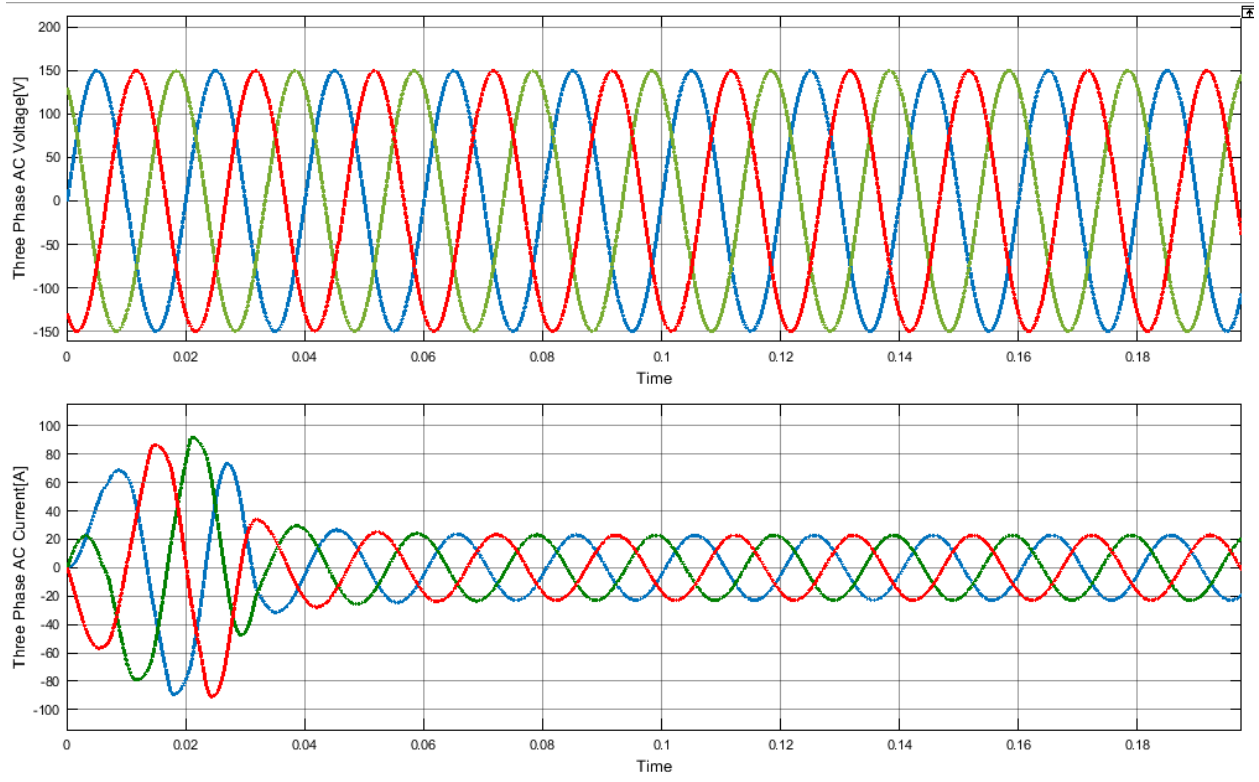
4.1. Bidirectional VSC as Active Front End (AFE) Rectifier:

The simulation for the bidirectional VSC as Active Front End (AFE) rectifier are shown in this section.

4.1.1. Regulation of DC link Voltage.



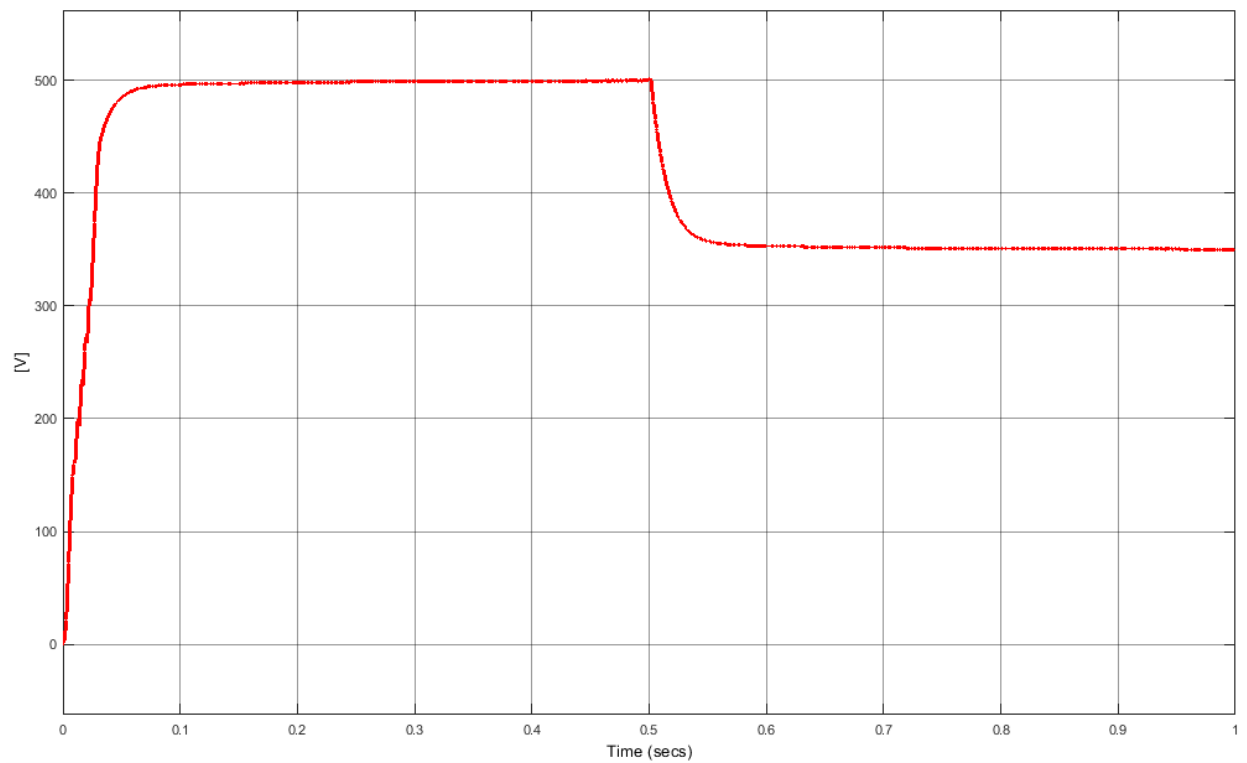
(a)



(b)

Figure 4.1 Simulation results of bidirectional VSC in Rectification mode: (a) DC link Voltage
 (b) Three phase grid Voltage (V) and Three Phase AC Grid Current (A)

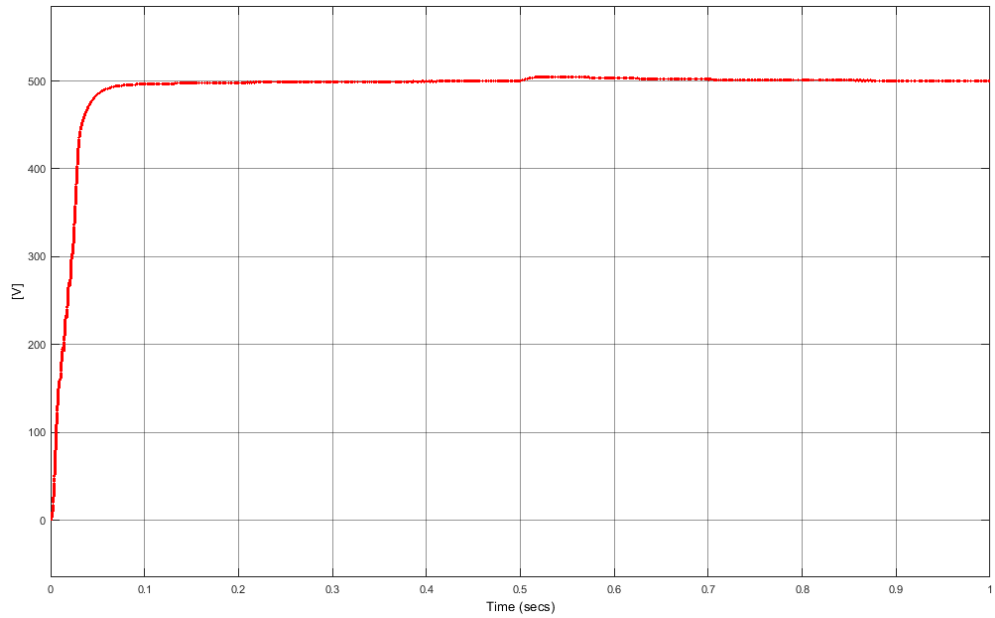
4.1.2. Step Change in DC link Voltage:



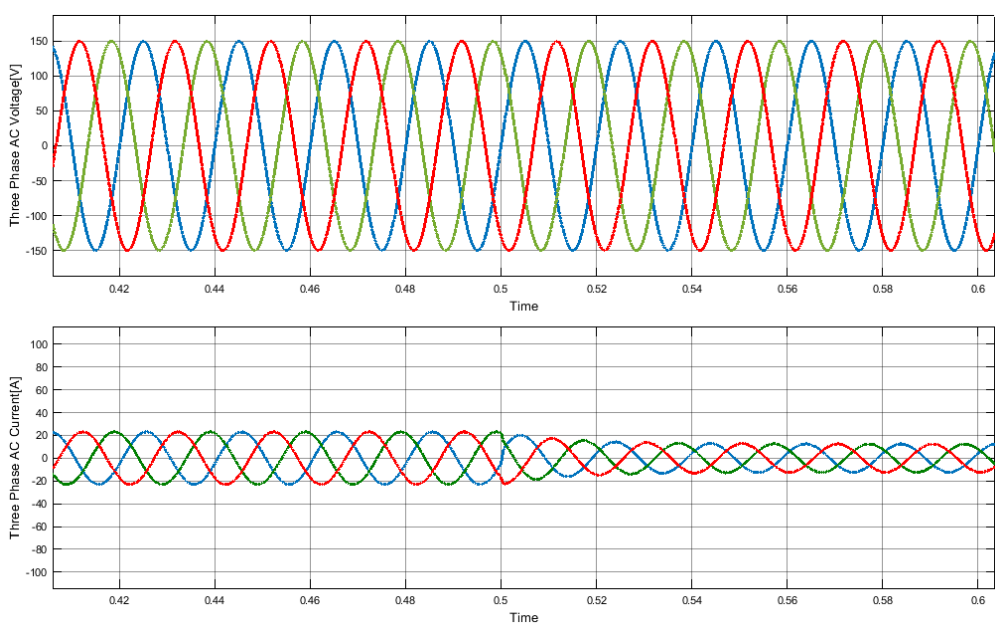
(a)

Figure 4.2 Simulation results of bidirectional VSC in Rectification mode: Step change in DC link Voltage from 500V to 350V at 0.5sec

4.1.3. Regulation of Load:



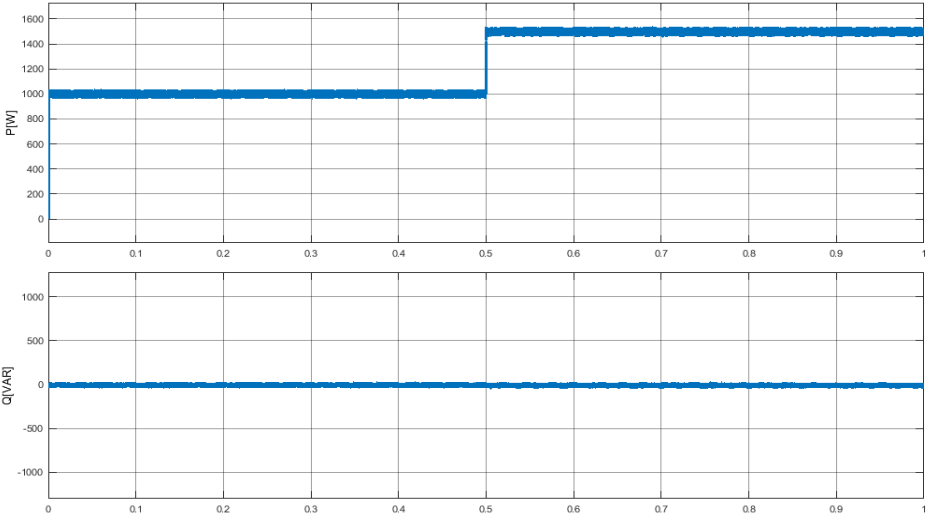
(a)



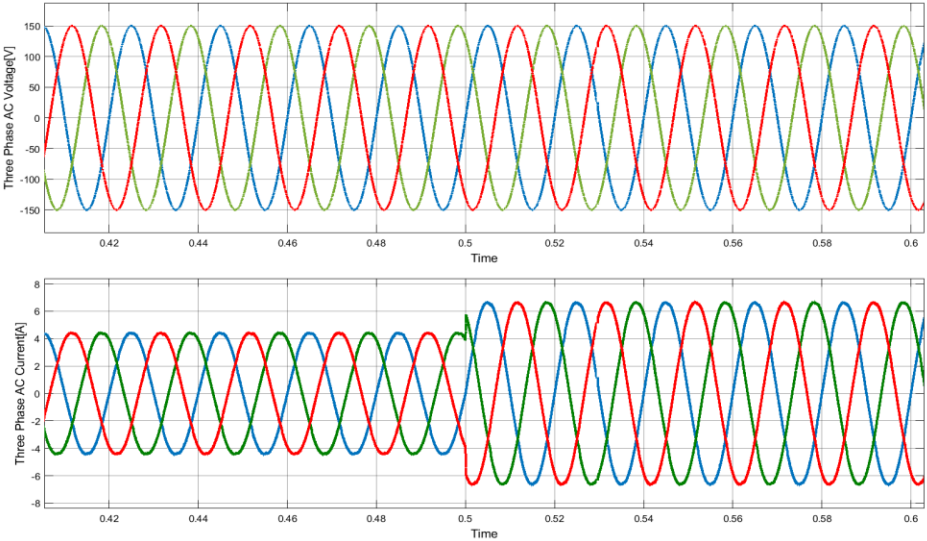
(b)

Figure 4.3 Simulation results of bidirectional VSC in Rectification mode: (a) Step change in load from 50 ohm to 100 ohm at 0.5sec (b) Three Phase grid Voltage (V) and Three Phase grid Current (A)

4.1.4. Regulation of power/Step Change in Power:



(a)



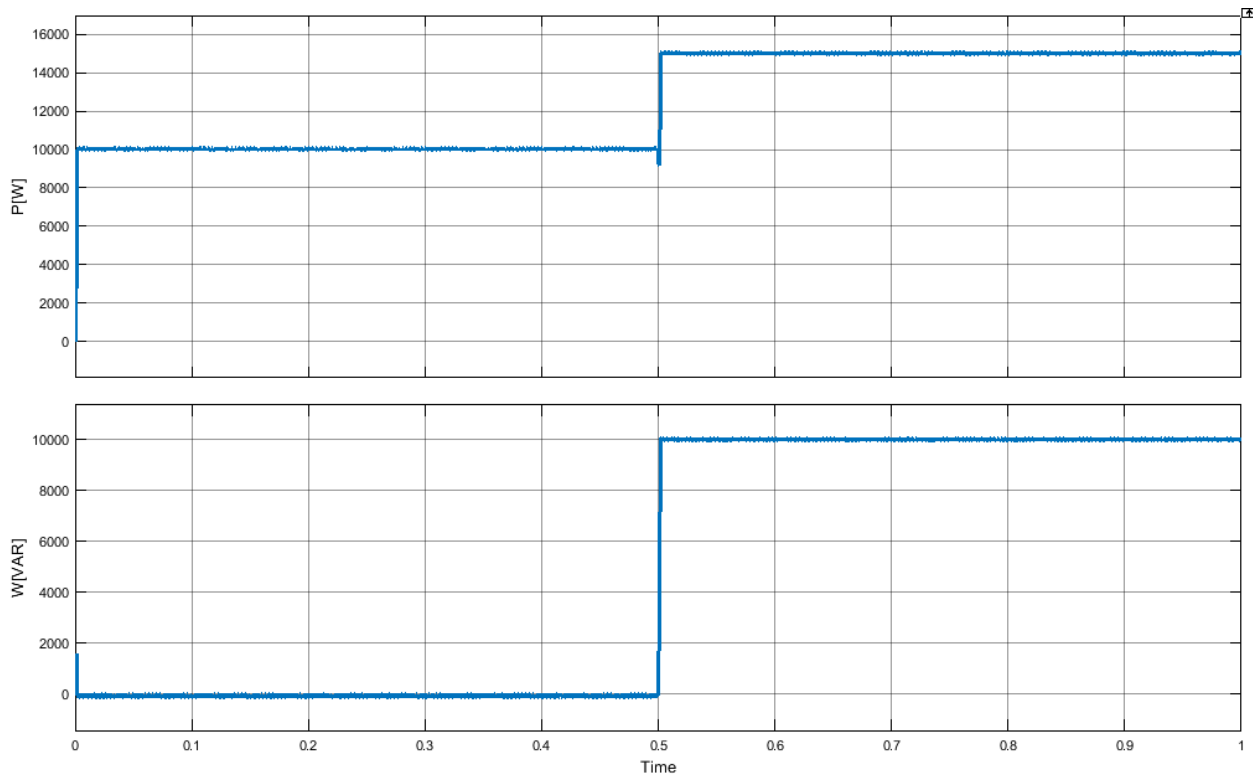
(b)

Figure 4.4 Simulation results of bidirectional VSC in Rectification mode: (a) Regulation of power/Step change in power on DC side from $P = 1\text{KW}$ to 1.5KW , $Q = 0\text{VAR}$ (b) Three Phase grid Voltage (V) and Three Phase grid Current (A)

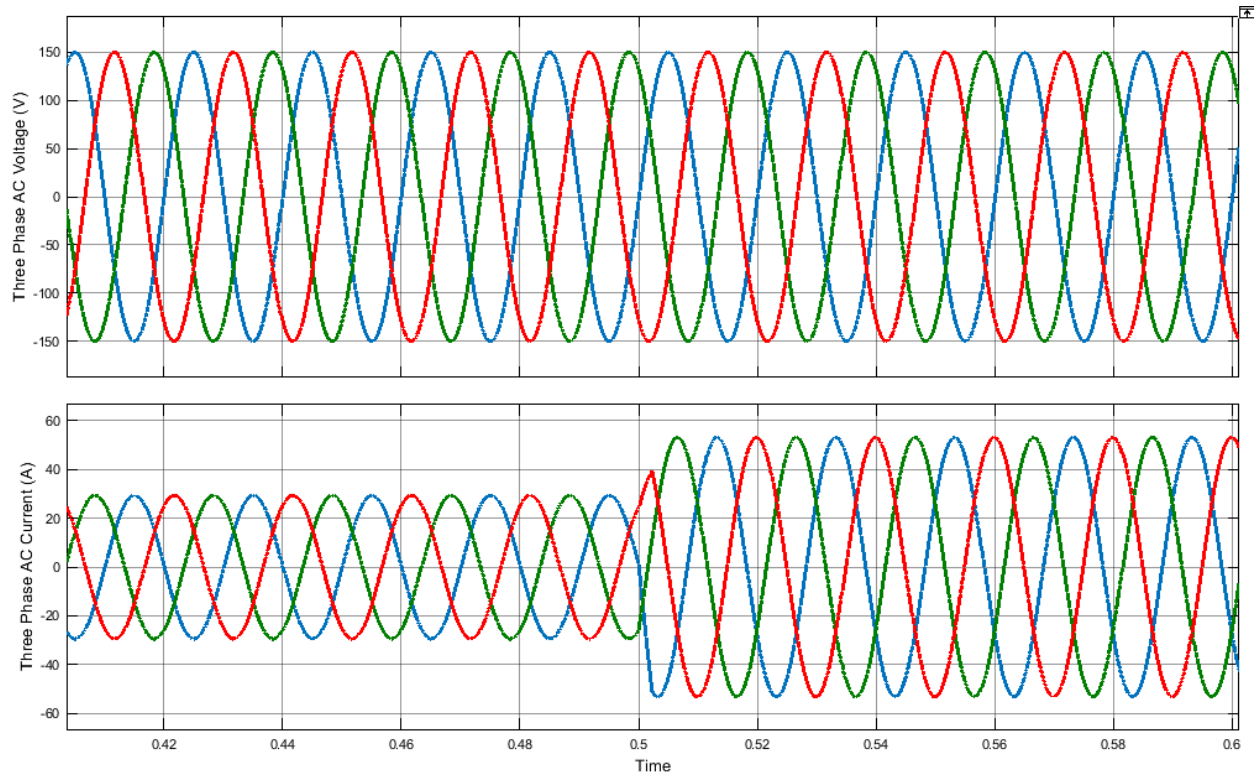
4.2. Bidirectional VSC as Voltage Source Inverter (Grid Connected Mode):

The simulation for the bidirectional VSC as inverter (Grid Connected Mode) rectifier are shown in this section.

4.2.1. Regulation of Power/Step Change in Power:



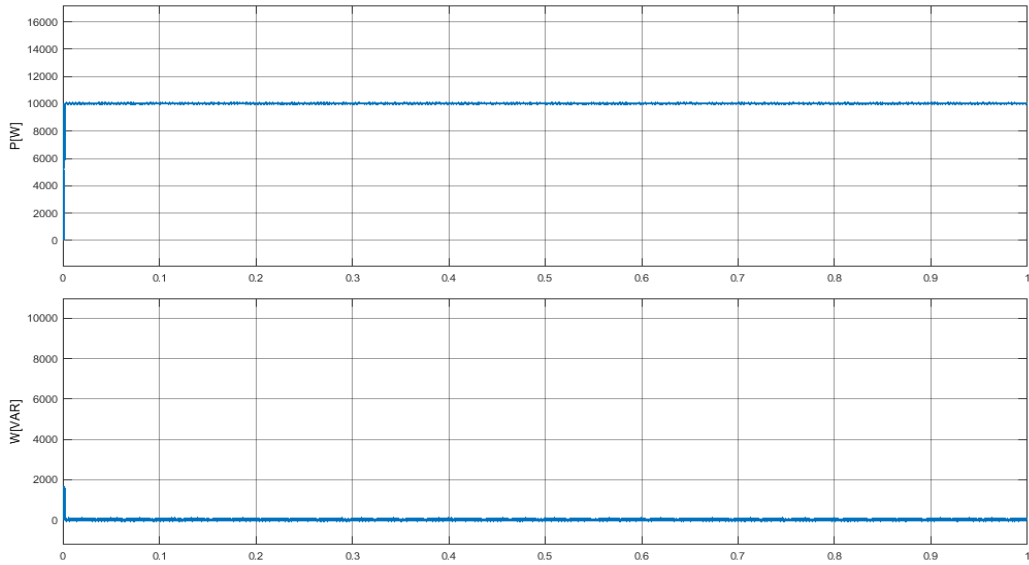
(a)



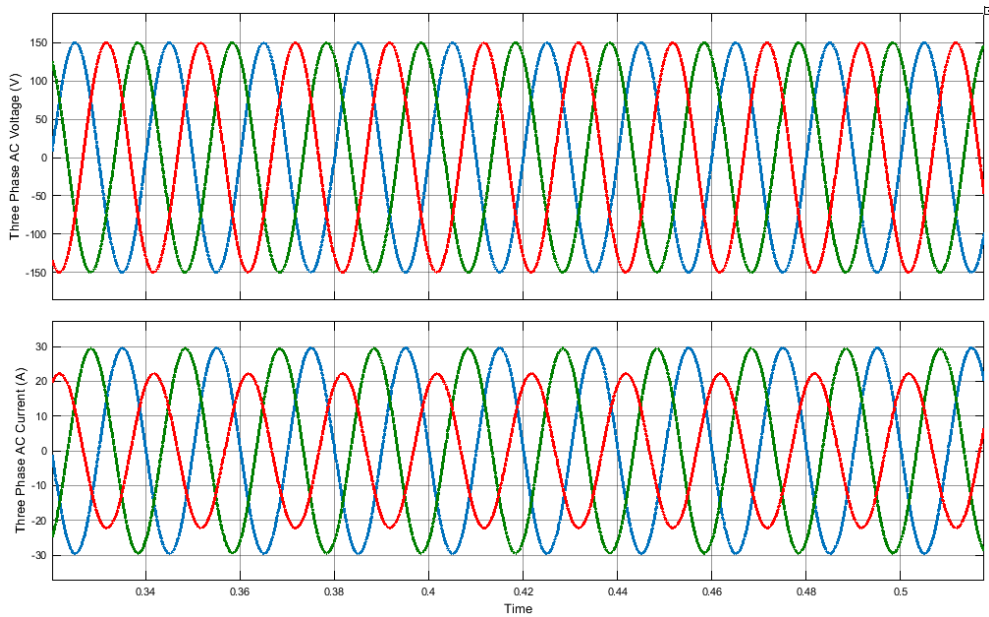
(b)

Figure 4.5 Simulation results of bidirectional VSC in Inverter (Grid Connected Mode): (a) Regulation of power/Step change in Power $P = 10\text{KW}$, $Q = 0\text{VAR}$ to $P = 15\text{KW}$, $Q = 10\text{kVAR}$
 (b) Three Phase AC Voltage (V) and Three Phase AC Current (A)

4.2.2. Unbalanced Linear load:



(a)



(b)

Figure 4.6 Simulation results of bidirectional VSC in Inverter (Grid Connected Mode): (a) Regulation of power $P = 10\text{KW}$, $Q = 0\text{VAR}$ (b) Three Phase AC Voltage (V) and Three Phase AC Current (A)

4.3. Bidirectional VSC as Voltage Source Inverter (Islanded Mode):

The simulation for the bidirectional VSC as inverter (islanded) are shown in this section.

4.3.1. Regulation of voltage and frequency:

(a)

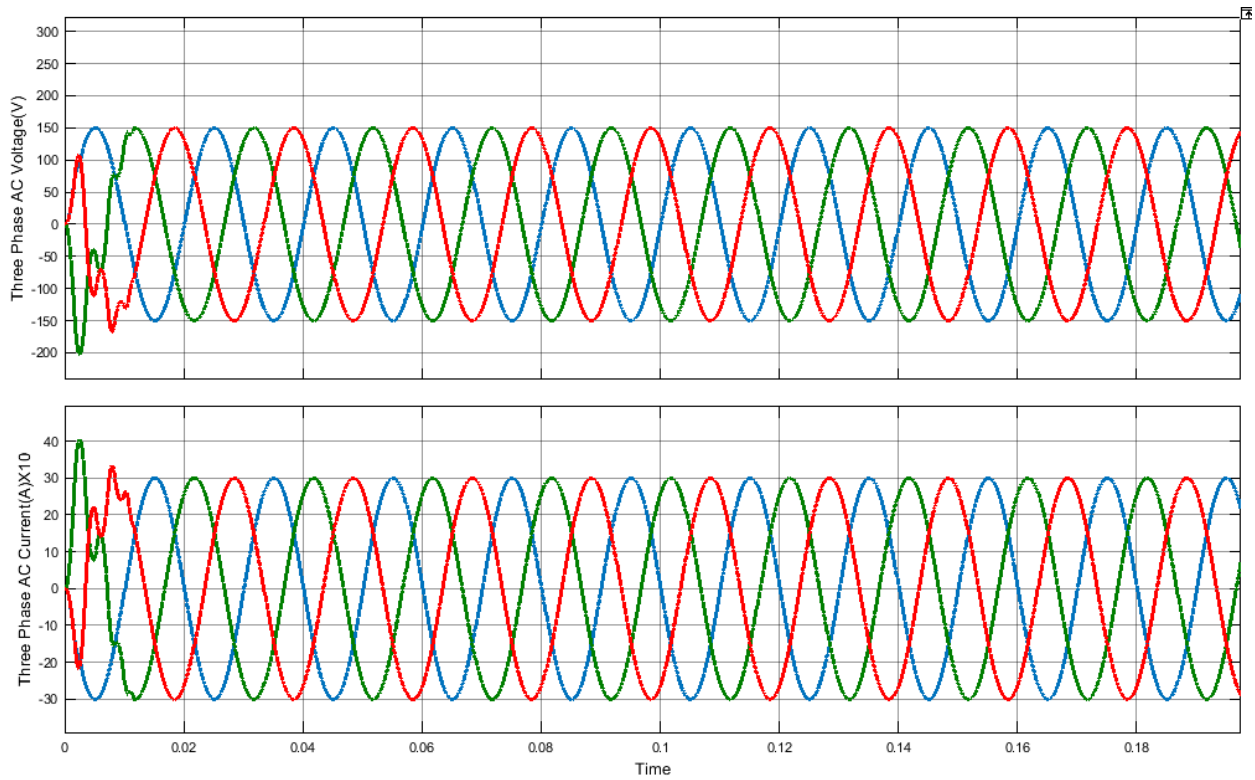
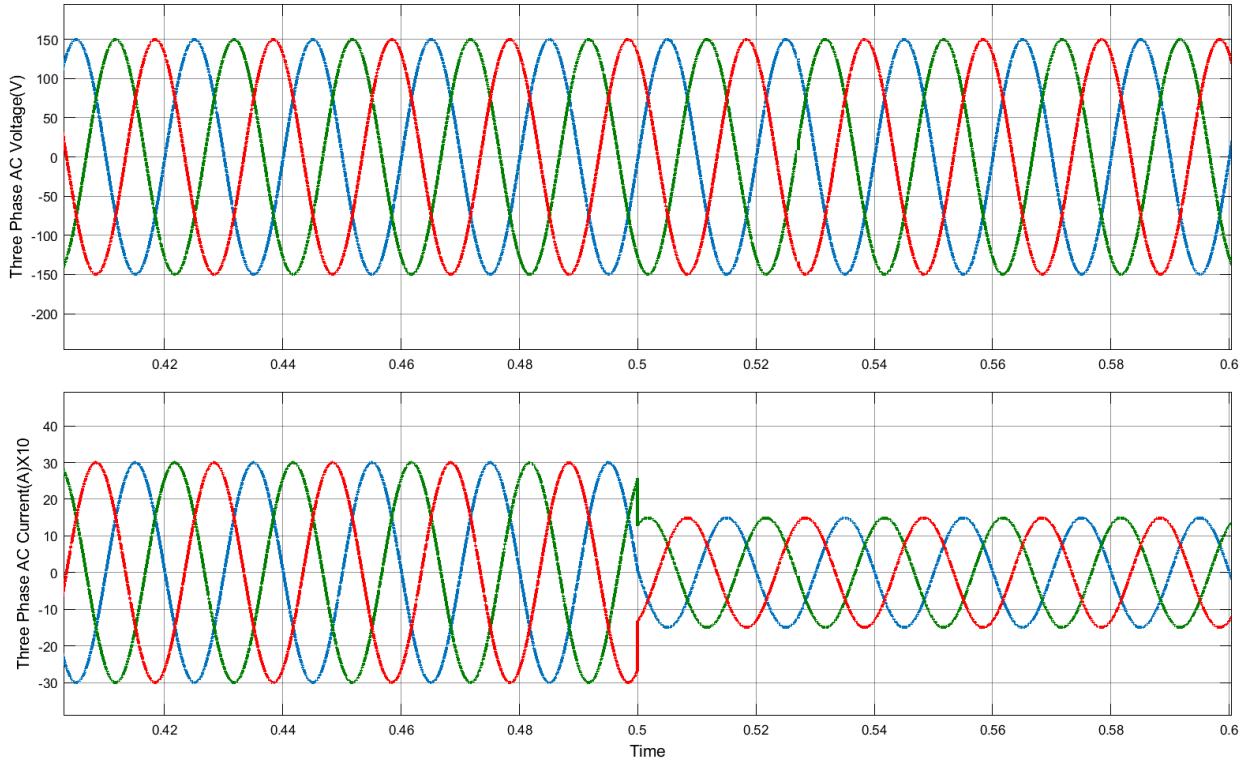


Figure 4.7 Simulation results of bidirectional VSC in Inverter (Islanded Mode): Three phase AC Grid Voltage and Three phase AC Grid Current (A) x10

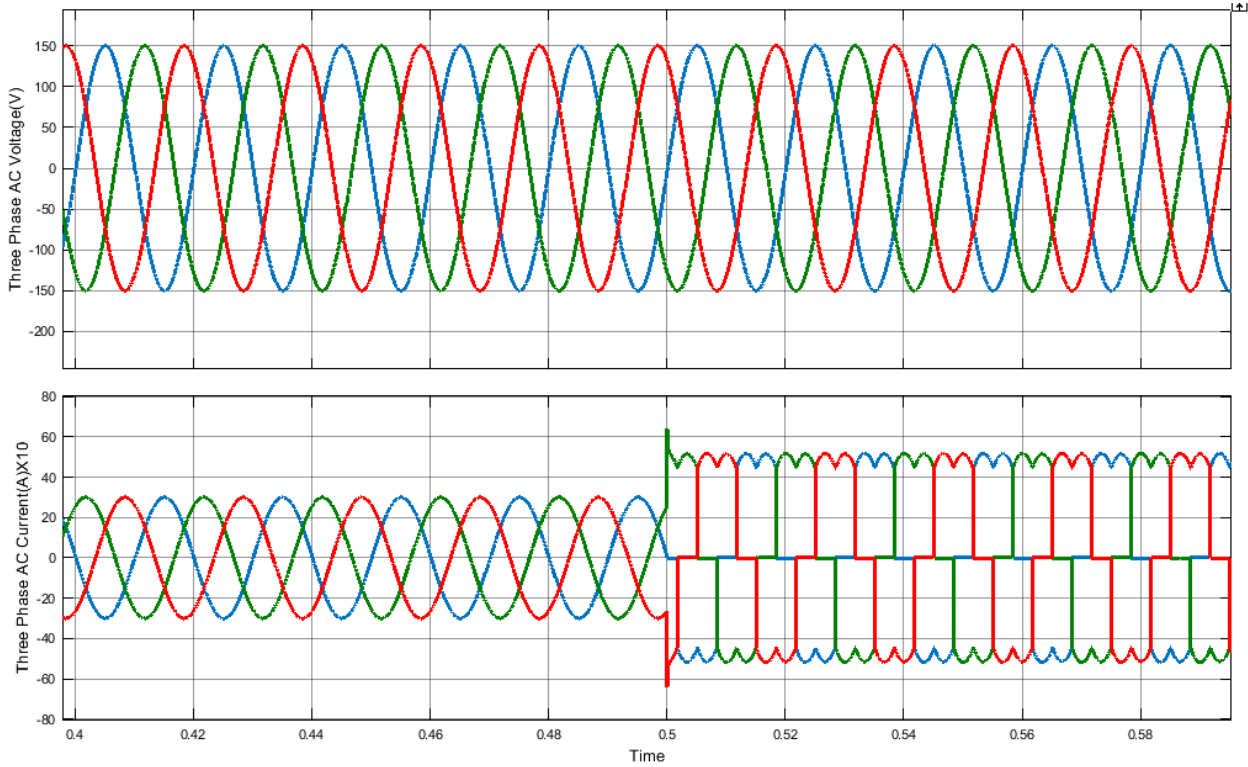
4.3.2. Step Change in Linear Load:



(a)

Figure 4.8 Simulation results of bidirectional VSC in Inverter (Islanded Mode): Three phase AC Grid Voltage and Three phase AC Grid Current (A) x10 for step change of load from 50 ohm to 100 ohm at 0.5sec

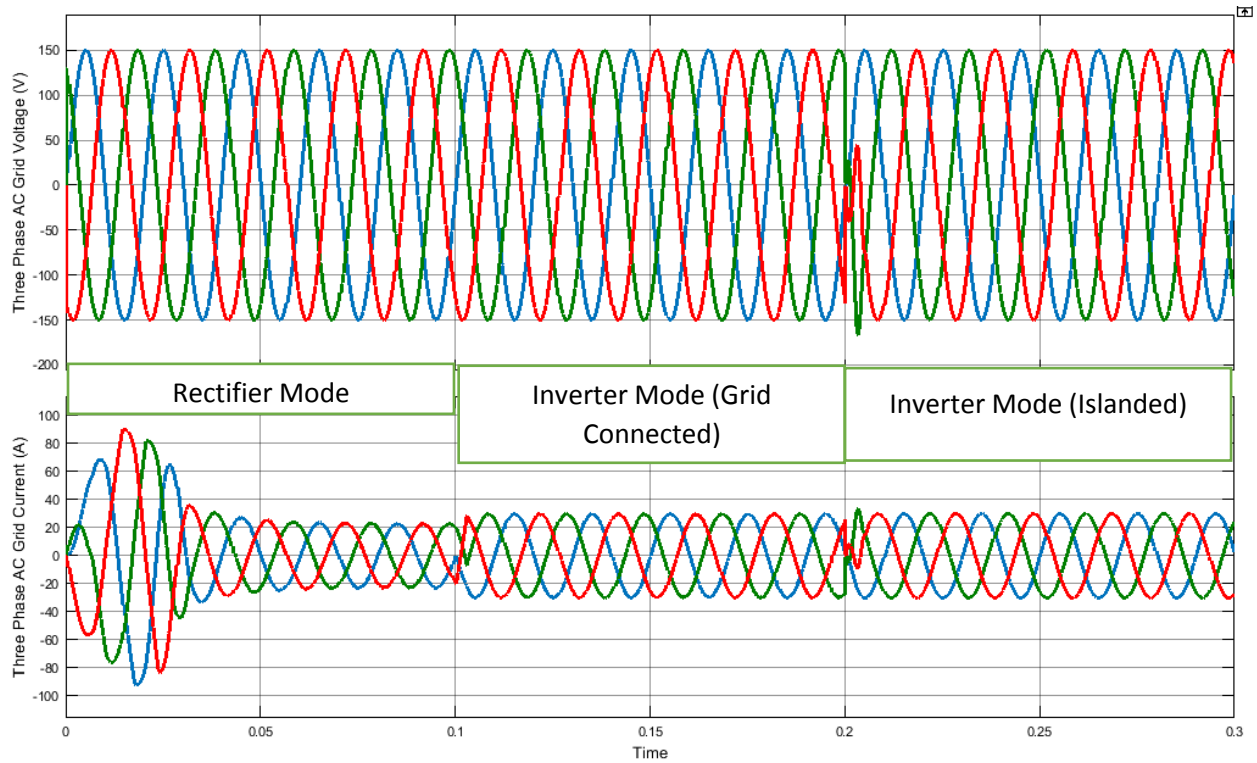
4.3.3. Non Linear Load:



(a)

Figure 4.9 Simulation results of bidirectional VSC in Inverter (Islanded Mode): Three phase AC Grid Voltage (V) and Three phase AC Grid Current (A) x10 when there is transition from linear load (50 ohm) to non linear load at 0.5sec

4.4. Transitions between modes of microgrid:



(a)

Figure 4.10 Simulation results of bidirectional VSC when there is transition between rectification mode and inverter mode: Three phase AC grid Voltage (V) and Three phase AC grid Current (A)

4.5. Comparative Analysis:

Table 4.2 % THD

Bidirectional Voltage Source Converter Mode	Parameter	% THD
As Active Front End Rectifier	Grid Current	0.56
As Voltage Source Inverter (Grid Connected Mode)	Grid Current	0.43
As Voltage Source Inverter (Islanded Mode)	Grid Voltage	0.50
As Voltage Source Inverter (Islanded Mode)	Grid Current	0.56
As Voltage Source (Inverter Islanded Mode) (Non Linear Load)	Grid Voltage	1

Table 4.3 Comparison between Conventional and Proposed Scheme (Inverter Mode)

Load Types	Voltage % THD(PI) [99]	Voltage %THD (Proposed MPC)
No Load	1.22	0.5
Balanced Resistive Load	1.22	0.5
Non-Linear Load	4.31	1

Table 4.4 Comparison between different control methods (Inverter Mode)

Reference	Control Technique	%Voltage THD Non-Linear Load	%Voltage THD Linear Load	Controller Complexity
[100]	PR	4.6	1.4	Low
[101]	SMC	2.66	-	High
[102]	PI	42	16	Low
[103]	Dead Beat	4.8	2.1	Medium
Proposed	FCS-MPC	1	0.5	Medium

Chapter 5

Conclusions and Future Work

CHAPTER 5. CONCLUSIONS

FUTURE WORK

AND

5.1. CONCLUSION:

In this study, Finite Control Set-Model Predictive Control (FCS-MPC) based three phase bidirectional AC/DC converter for hybrid microgrid is implemented. It can operate either in rectification mode or inverter mode. In rectification mode, it maintains voltage on the DC side or regulates power on the DC side. In inverter mode, it can further operate in two modes, islanded mode and grid connected mode. In the grid connected mode, national grid controls the voltage and frequency of the microgrid while power is controlled by the bidirectional VSC. In the islanded mode, bidirectional VSC controls the voltage, frequency of a microgrid and also fulfills the local demand. Results are verified using MATLAB/SIMULINK under different case studies showing that the proposed technique has good dynamic response, effective and robust for both unbalanced and nonlinear load conditions. In addition, the %THD of voltage and current are within limits. The percent Voltage THD in case of proposed scheme is 0.5% and 1% for linear and nonlinear load which is better than all other techniques.

5.2. FUTURE WORK:

- Experimental verification of proposed controlled scheme.

REFERENCES

1. G. Pepermans, J. Driesen, D. Haeseldonckx, R. Belmans, and W. D'haeseleer, "Distributed generation: Definition, benefits and issues," *Energy Policy*, vol. 33, no. 6, pp. 787–798, **2005**.
2. T. C. Green and M. Prodanovic, "Control of inverter-based micro-grids," *Electr. Power Syst. Res. Distrib. Generation*, vol. 77, no. 9, pp. 1204–1213, **2007**.
3. E. Planas, A. Gil-De-Muro, J. Andreu, I. Kortabarria, and I. Martínez De Alegría, "General aspects, hierarchical controls and droop methods in microgrids: A review," *Renewable and Sustainable Energy Reviews*, vol. 17, pp. 147–159, **Jan-2013**.
4. J. J. Justo, F. Mwasilu, J. Lee, and J. W. Jung, "AC-microgrids versus DC-microgrids with distributed energy resources: A review," *Renewable and Sustainable Energy Reviews*, vol. 24, Elsevier, pp. 387–405, **Aug-2013**.
5. E. Hossain, E. Kabalci, R. Bayindir, and R. Perez, "Microgrid testbeds around the world: State of art," *Energy Convers. Manag.*, vol. 86, pp. 132–153, **Oct. 2014**.
6. N. Eghtedarpour and E. Farjah, "Power Control and Management in a Hybrid AC/DC Microgrid," *IEEE Trans. Smart Grid*, vol. 5, no. 3, pp. 1494–1505, **May 2014**.
7. D. J. Hammerstrom, "AC Versus DC Distribution Systems Did We Get it Right?," in *IEEE Power Engineering Society General Meeting*, **2007**, pp. 1–5.
8. Z. Jiang and X. Yu, "Hybrid DC- and AC-Linked Microgrids: Towards Integration of Distributed Energy Resources," in *IEEE Energy 2030 Conference*, **2008**, pp. 1–8.
9. R. A. Kaushik and N. M. Pindoriya, "A hybrid AC-DC microgrid: Opportunities & key issues in implementation," in *International Conference on Green Computing Communication and Electrical Engineering (ICGCCEE)*, **2014**, pp. 1–6.
10. I. Patrao, E. Figueres, G. Garcerá, and R. González-Medina, "Microgrid architectures for low voltage distributed generation," *Renew. Sustain. Energy Rev.*, vol. 43, pp. 415–424, **Mar. 2015**.
11. M. Starke, L. M. Tolbert, and B. Ozpineci, "AC vs. DC distribution: A loss comparison," in *IEEE/PES Transmission and Distribution Conference and Exposition*, **2008**, pp. 1–7.

12. P. Wang, L. Goel, X. Liu, and F. H. Choo, "Harmonizing AC and DC: A Hybrid AC/DC future grid solution," *IEEE Power Energy Mag.*, vol. 11, no. 3, pp. 76–83, **May 2013**.
13. X. Zhu, X. Han, W. Qin, and P. Wang, "Past, today and future development of micro-grids in China," *Renew. Sustain. Energy Rev.*, vol. 42, pp. 1453–1463, **Feb. 2015**.
14. N. W. A. Lidula and A. D. Rajapakse, "Microgrids research: A review of experimental microgrids and test systems," *Renewable and Sustainable Energy Reviews*, vol. 15, no. 1. Elsevier Ltd, pp. 186–202, **Jan-2011**.
15. M. Soshinskaya, W. H. J. Graus, J. M. Guerrero, and J. C. Vasquez, "Microgrids: experiences, barriers and success factors," *Renew. Sustain. Energy Rev.*, vol. 40, pp. 659–672, **Dec. 2014**.
16. E. Hossain, E. Kabalci, R. Bayindir, and R. Perez, "Microgrid testbeds around the world: State of art," *Energy Convers. Manag.*, vol. 86, pp. 132–153, **Oct. 2014**.
17. D. J. Hammerstrom, "AC Versus DC Distribution Systems Did We Get it Right?," in *IEEE Power Engineering Society General Meeting*, **2007**, pp. 1–5.
18. E. Planas, J. Andreu, J. I. Gárate, I. Martínez de Alegría, and E. Ibarra, "AC and DC technology in microgrids: A review," *Renew. Sustain. Energy Rev.*, vol. 43, pp. 726–749, **Mar. 2015**.
19. E. Planas, A. Gil-De-Muro, J. Andreu, I. Kortabarria, and I. Martínez De Alegría, "General aspects, hierarchical controls and droop methods in microgrids: A review," *Renewable and Sustainable Energy Reviews*, vol. 17. pp. 147–159, **Jan-2013**.
20. J. J. Justo, F. Mwasilu, J. Lee, and J. W. Jung, "AC-microgrids versus DC-microgrids with distributed energy resources: A review," *Renewable and Sustainable Energy Reviews*, vol. 24. Elsevier, pp. 387–405, **Aug-2013**.
21. D. J. Hammerstrom, "AC Versus DC Distribution Systems Did We Get it Right?," in *IEEE Power Engineering Society General Meeting*, 2007, pp. 1–5.
22. I. Patrao, E. Figueres, G. Garcerá, and R. González-Medina, "Microgrid architectures for low voltage distributed generation," *Renew. Sustain. Energy Rev.*, vol. 43, pp. 415–424, **Mar. 2015**.
23. M. Starke, L. M. Tolbert, and B. Ozpineci, "AC vs. DC distribution: A loss comparison," in *IEEE/PES Transmission and Distribution Conference and Exposition*, **2008**, pp. 1–7.

24. R. A. Kaushik and N. M. Pindoriya, "A hybrid AC-DC microgrid: Opportunities & key issues in implementation," in *International Conference on Green Computing Communication and Electrical Engineering (ICGCCEE)*, **2014**, pp. 1–6.
25. I. Patrao, E. Figueres, G. Garcerá, and R. González-Medina, "Microgrid architectures for low voltage distributed generation," *Renew. Sustain. Energy Rev.*, vol. 43, pp. 415–424, **Mar. 2015**.
26. Z. Jiang and X. Yu, "Hybrid DC- and AC-Linked Microgrids: Towards Integration of Distributed Energy Resources," in *IEEE Energy 2030 Conference*, **2008**, pp. 1–8
27. P. Wang, L. Goel, X. Liu, and F. H. Choo, "Harmonizing AC and DC: A Hybrid AC/DC future grid solution," *IEEE Power Energy Mag.*, vol. 11, no. 3, pp. 76–83, **May 2013**.
28. E. Planas, J. Andreu, J. I. Gárate, I. Martínez de Alegría, and E. Ibarra, "AC and DC technology in microgrids: A review," *Renew. Sustain. Energy Rev.*, vol. 43, pp. 726–749, **Mar. 2015**.
29. J. Rocabert, A. Luna, F. Blaabjerg, and P. Rodríguez, "Control of power converters in AC microgrids," *IEEE Trans. Power Electron.*, vol. 27, no. 11, pp. 4734–4749, **Nov. 2012**.
30. B. Singh, S. Gairola, B. N. Singh, A. Chandra, and K. Al-Haddad, "Multipulse AC–DC converters for improving power quality: a review," *IEEE Trans. Power Electron.*, vol. 23, pp. 260–281, 2008.
31. B. Singh, B. N. Singh, A. Chandra, K. Al-Haddad, A. Pandey, and D. P. Kothari, "A review of three-phase improved power quality AC-DC converters," *IEEE Trans. Ind. Electron.*, vol. 51, pp. 641–660, 2004.
32. J. Dannehl, C. Wessels, and F. W. Fuchs, "Limitations of VoltageOriented PI Current Control of Grid-Connected PWM Rectifiers With LCL Filters," *IEEE Trans. Ind. Electron.*, vol. 56, 2009.
33. P. Verdelho and G. Marques, "DC voltage control and stability analysis of PWM-voltage-type reversible rectifiers," *IEEE Trans. Ind. Electron.*, vol. 45, pp. 263–273, 1998.
34. P. Verdelho and G. Marques, "DC voltage control and stability analysis of PWM-voltage-type reversible rectifiers," *IEEE Trans. Ind. Electron.*, vol. 45, pp. 263–273, **1998**.

35. H. Li, F. Li, Y. Xu, D. T. Rizy, and J. D. Kueck, "Adaptive voltage control with distributed energy resources: Algorithm, theoretical analysis, simulation, and field test verification," *IEEE Transactions on Power Systems*, vol. 25, pp. 1638-1647, **2010**.
36. Y. Xu and F. Li, "Adaptive PI control of STATCOM for voltage regulation," *IEEE transactions on power delivery*, vol. 29, pp. 1002-1011, **2014**.
37. E. Twining and D. G. Holmes, "Grid current regulation of a three-phase voltage source inverter with an LCL input filter," *IEEE Transactions on Power Electronics*, vol. 18, pp. 888-895, **2003**.
38. G. Shen, D. Xu, L. Cao, and X. Zhu, "An improved control strategy for grid-connected voltage source inverters with an LCL filter," *IEEE Transactions on Power Electronics*, vol. 23, pp. 1899-1906, **2008**.
39. D. M. Brod and D. W. Novotny, "Current control of VSI-PWM inverters," *IEEE Transactions on Industry Applications*, pp. 562-570, **1985**.
40. R. Teodorescu, F. Blaabjerg, U. Borup, and M. Liserre, "A new control structure for grid-connected LCL PV inverters with zero steady-state error and selective harmonic compensation," in *Applied Power Electronics Conference and Exposition, 2004. APEC'04. Nineteenth Annual IEEE*, **2004**, pp. 580-586.
41. J. Holtz, "Pulsewidth modulation for electronic power conversion," *Proceedings of the IEEE*, vol. 82, pp. 1194-1214, **1994**.
42. I. Takahashi and T. Noguchi, "A new quick-response and high-efficiency control strategy of an induction motor," *IEEE Transactions on Industry applications*, pp. 820-827, **1986**.
43. T. Ohnishi, "Three phase PWM converter/inverter by means of instantaneous active and reactive power control," in *Industrial Electronics, Control and Instrumentation, 1991. Proceedings. IECON'91., 1991 International Conference on*, **1991**, pp. 819-824.
44. M. Malinowski, M. P. Kazmierkowski, and A. M. Trzynadlowski, "A comparative study of control techniques for PWM rectifiers in AC adjustable speed drives," *IEEE Trans. Power Electron.*, vol. 18, pp. 1390-1396, **2003**.
45. D. Zhi, L. Xu, and B. W. Williams, "Improved direct power control of grid-connected DC/AC converters," *IEEE Transactions on Power Electronics*, vol. 24, pp. 1280-1292, **2009**.

46. T. Noguchi, H. Tomiki, S. Kondo, and I. Takahashi, "Direct power control of PWM converter without power-source voltage sensors," *IEEE Transactions on Industry Application*, vol. 34, pp. 473-479, **1998**.
47. I. Takahashi and Y. Ohmori, "High-performance direct torque control of an induction motor," *IEEE Transactions on Industry Application*, vol. 25, pp. 257-264, **1989**.
48. C. Lascu, I. Boldea, and F. Blaabjerg, "A modified direct torque control for induction motor sensorless drive," *IEEE Transactions on Industry Application*, vol. 36, pp. 122-130, **2000**.
49. S. Vazquez, J. A. Sanchez, J. M. Carrasco, J. I. Leon, and E. Galvan, "A model-based direct power control for three-phase power converters," *IEEE Trans. Ind. Electron.*, vol. 55, pp. 1647-1657, **2008**.
50. D. Zhi, L. Xu, B. W. Williams, L. Yao, and M. Bazargan, "A new direct power control strategy for grid connected voltage source converters," in *Proc. Int. Conf. Elect. Machines and Syst. (ICEMS)*, **2008**, pp. 1157-1162.
51. A. Bouafia, F. Krim, and J.-P. Gaubert, "Fuzzy-logicbased switching state selection for direct power control of three-phase PWM rectifier," *IEEE Trans. Ind. Electron.*, vol. 56, pp. 1984-1992, **2009**.
52. J. Hu, L. Shang, Y. He, and Z. Zhu, "Direct active and reactive power regulation of grid-connected DC/AC converters using sliding mode control approach," *IEEE Trans. Power Electron.*, vol. 26, pp. 210-222, **2011**
53. J. Y. Hung, W. Gao, and J. C. Hung, "Variable structure control: A survey," *IEEE transactions on industrial electronics*, vol. 40, pp. 2-22, **1993**.
54. R. Guzman, L. G. de Vicuna, A. Camacho, J. Matas, M. Castilla, and J. Miret, "Active damping control for a three phase grid-connected inverter using sliding mode control," in *Industrial Electronics Society, IECON 2013-39th Annual Conference of the IEEE*, **2013**, pp. 382-387.
55. C.-C. Lee, "Fuzzy logic in control systems: fuzzy logic controller. I," *IEEE Transactions on systems, man, and cybernetics*, vol. 20, pp. 404-418, **1990**.

56. M. Hannan, Z. A. Ghani, A. Mohamed, and M. N. Uddin, "Real-time testing of a fuzzy-logic-controller-based grid-connected photovoltaic inverter system," *IEEE Transactions on Industry Applications*, vol. 51, pp. 4775-4784, **2015**.
57. B. K. Bose, *Power electronics and motor drives: advances and trends*: Elsevier, **2010**.
58. J. M. Maciejowski, *Predictive control: with constraints*: Pearson education, **2002**.
59. A. Propoi, "Use of linear programming methods for synthesizing sampled-data automatic systems," *Autumn. Remote Control*, vol. 24, pp. 837-844, **1963**.
60. M. Morari and J. H. Lee, "Model predictive control: past, present and future," *Computers & Chemical Engineering*, vol. 23, pp. 667-682, **1999**.
61. C. E. Garcia, D. M. Prett, and M. Morari, "Model predictive control: theory and practice—a survey," *Automatica*, vol. 25, pp. 335-348, **1989**.
62. J. Holtz, "A predictive controller for the stator current vector of ac machines fed from a switched voltage source," *Proc. of IEE of Japan IPEC-Tokyo'83*, pp. 1665-1675, **1983**.
63. P. Cortés, M. P. Kazmierkowski, R. M. Kennel, D. E. Quevedo, and J. Rodríguez, "Predictive control in power electronics and drives," *IEEE Transactions on industrial electronics*, vol. 55, pp. 4312-4324, **2008**.
64. J. Rodriguez and P. Cortes, *Predictive control of power converters and electrical drives* vol. 40: John Wiley & Sons, **2012**.
65. P. Mutschler, "A new speed-control method for induction motors," in *Proc. Conf. Rec. PCIM*, **1998**, pp. 131-136.
66. O. Kukrer, "Discrete-time current control of voltage-fed three-phase PWM inverters," *IEEE Transactions on Power Electronics*, vol. 11, pp. 260-269, **1996**.
67. E. F. Camacho and C. Bordons, "Model predictive control (advanced textbooks in control and signal processing)," **1999**.
68. S. Kouro, P. Cortés, R. Vargas, U. Ammann, and J. Rodríguez, "Model predictive control—A simple and powerful method to control power converters," *IEEE Transactions on Industrial Electronics*, vol. 56, pp. 1826-1838, **2009**.
69. P. Cortes, A. Wilson, S. Kouro, J. Rodriguez, and H. Abu-Rub, "Model predictive control of multilevel cascaded H-bridge inverters," *IEEE Transactions on Industrial Electronics*, vol. 57, pp. 2691-2699, **2010**.

70. V. Yaramasu and B. Wu, "Predictive control of a three-level boost converter and an NPC inverter for high-power PMSG-based medium voltage wind energy conversion systems," *IEEE Transactions on Power Electronics*, vol. 29, pp. 5308-5322, **2014**.
71. S. Vazquez, J. Rodriguez, M. Rivera, L. G. Franquelo, and M. Norambuena, "Model predictive control for power converters and drives: Advances and trends," *IEEE Transactions on Industrial Electronics*, vol. 64, pp. 935-947, **2017**.
72. D. Mayne and J. Rawlings, "Model predictive control: theory and design," *Madison, WI: Nob Hill Publishing, LCC*, **2009**.
73. E. F. Camacho and C. B. Alba, *Model predictive control: Springer Science & Business Media*, **2013**.
74. S. J. Qin and T. A. Badgwell, "A survey of industrial model predictive control technology," *Control engineering practice*, vol. 11, pp. 733-764, **2003**.
75. M. R. Arahal, F. Barrero, M. G. Ortega, and C. Martin, "Harmonic analysis of direct digital control of voltage inverters," *Mathematics and Computers in Simulation*, vol. 130, pp. 155-166, **2016**.
76. J. Rodriguez, J. Pontt, C. A. Silva, P. Correa, P. Lezana, P. Cortés, *et al.*, "Predictive current control of a voltage source inverter," *IEEE transactions on industrial electronics*, vol. 54, pp. 495-503, **2007**.
77. S. Kwak and J.-C. Park, "Model-predictive direct power control with vector preselection technique for highly efficient active rectifiers," *IEEE Transactions on Industrial Informatics*, vol. 11, pp. 44-52, **2015**.
78. P. Cortés, J. Rodríguez, D. E. Quevedo, and C. Silva, "Predictive current control strategy with imposed load current spectrum," *IEEE Transactions on Power Electronics*, vol. 23, pp. 612-618, **2008**.
79. T.-T. Nguyen, H.-J. Yoo, and H.-M. Kim, "Application of model predictive control to BESS for microgrid control," *Energies*, vol. 8, pp. 8798-8813, **2015**.
80. N. Naeiji, M. Hamzeh, and A. R. Kian, "A modified model predictive control method for voltage control of an inverter in islanded microgrids," in *Power Electronics, Drives Systems & Technologies Conference (PEDSTC), 2015 6th*, **2015**, pp. 555-560.

81. Han, S. K. Solanki, and J. Solanki, "Coordinated predictive control of a wind/battery microgrid system," *IEEE Journal of emerging and selected topics in power electronics*, vol. 1, pp. 296-305, **2013**.
82. G. Lou, W. Gu, Y. Xu, M. Cheng, and W. Liu, "Distributed MPC-based secondary voltage control scheme for autonomous droop-controlled microgrids," *IEEE Transactions on Sustainable Energy*, vol. 8, pp. 792-804, **2017**.
83. Kwak, S.; Park, J.-C. Model-predictive direct power control with vector preselection technique for highly efficient active rectifiers. *IEEE Trans. Ind. Inform.* **2015**, *11*, 44–52.
84. Cortés, P.; Rodríguez, J.; Quevedo, D.E.; Silva, C. Predictive current control strategy with imposed load current spectrum. *IEEE Trans. Power Electron.* **2008**, *23*, 612–618.
85. Nguyen, T.-T.; Yoo, H.-J.; Kim, H.-M. Application of model predictive control to BESS for microgrid control. *Energies* **2015**, *8*, 8798–8813.
86. Arahal, M.R.; Barrero, F.; Durán, M.J.; Ortega, M.G.; Martín, C. Trade-offs analysis in predictive current control of multi-phase induction machines. *Control Eng. Pract.* **2018**, *81*, 105–113.
87. Lim, C.S.; Levi, E.; Jones, M.; Rahim, N.A.; Hew, W.P. FCS-MPC-based current control of a five-phase induction motor and its comparison with PI-PWM control. *IEEE Trans. Ind. Electron.* **2014**, *61*, 149–163.
88. Arahal, M.R.; Barrero, F.; Ortega, M.G.; Martín, C. Harmonic analysis of direct digital control of voltage inverters. *Math. Comput. Simul.* **2016**, *130*, 155–166.
89. Yaramasu, V.; Rivera, M.; Narimani, M.; Wu, B.; Rodriguez, J. Model predictive approach for a simple and effective load voltage control of four-leg inverter with an output LC filter. *IEEE Trans. Ind. Electron.* **2014**, *61*, 5259–5270.
90. Nauman, M.; Hasan, A. Efficient implicit model-predictive control of a three-phase inverter with an output LC filter. *IEEE Trans. Power Electron.* **2016**, *31*, 6075–6078.
91. N. Mohan, T. Underland, and W. Robbins, *Power Electronics*, 2nd ed. John Wiley & Sons, Inc. 1995.
92. J. Rodríguez, J. Dixon, J. Espinoza, J. Pont, and P. Lezana, "PWM regenerative rectifiers: state of the art," *IEEE Transactions on Industrial Electronics*, vol. 52, no. 1, pp. 5–22, February **2005**.

93. M. Malinowski, M. P. Kazmierkowski, and A. M. Trzynadlowski, "A comparative study of control techniques for PWM rectifiers in AC adjustable speed drives," *IEEE Transactions on Power Electronics*, vol. 18, no. 6, pp. 1390–1396, **November 2003**.
94. T. G. Habetler, "A space vector-based rectifier regulator for AC/DC/AC converters," *IEEE Transactions on Power Electronics*, vol. 8, no. 1, pp. 30–36, **January 1993**.
95. T. Noguchi, H. Tomiki, S. Kondo, and I. Takahashi, "Direct power control of PWM converter without power-source voltage sensors," *IEEE Transactions on Industry Applications*, vol. 34, no. 3, pp. 473–479, **May/June 1998**.
96. M. Malinowski, M. Jasinski, and M. P. Kazmierkowski, "Simple direct power control of three-phase PWM rectifier using space-vector modulation (DPC-SVM)," *IEEE Transactions on Industrial Electronics*, vol. 51, no. 2, pp. 447–454, **April 2004**.
97. H. Akagi, E. Watanabe, and M. Aredes, *Instantaneous Power Theory and Applications to Power Conditioning*, IEEE Press Series on Power Engineering. John Wiley & Sons, Inc. **2007**.
98. P. Cortes, J. Rodr ´ ıguez, P. Antoniewicz, and M. Kazmierkowski, "Direct power control of an AFE using predictive control," *IEEE Transactions on Power Electronics*, vol. 23, no. 5, pp. 2516–2523, September **2008**.
99. Hussain Sarwar Khan, Muhammad Ali, Muhammad Aamir and Asad Waqar "Finite Control Set Model Predictive Control for Parallel Connected Online UPS System under unbalanced and non linear load" in *Energies* · February **2019**.
100. Hasanzadeh, A.; Onar, O.C.; Mokhtari, H.; Khaligh, A. A proportional-resonant controller-based wireless control strategy with a reduced number of sensors for parallel-operated UPSs. *IEEE Trans. Power Deliv.* **2010**, 25, 468–478.
101. Komurcugil, H. Rotating-sliding-line-based sliding-mode control for single-phase UPS inverters. *IEEE Trans. Ind. Electron.* **2012**, 59, 3719–3726/
102. Loh, P.C.; Newman, M.J.; Zmood, D.N.; Holmes, D.G. A comparative analysis of multiloop voltage regulation strategies for single and three-phase UPS systems. *IEEE Trans. Power Electron.* **2003**, 18, 1176–1185.
103. Mattavelli, P. An improved deadbeat control for UPS using disturbance observers. *IEEE Trans. Ind. Electron.* **2005**, 52, 206–212.

